In presenting the dissertation as a partial fulfillment of the requirements for an advanced degree from the Georgia Institute of Technology, I agree that the Library of the Institute shall make it available for inspection and circulation in accordance with its regulations governing materials of this type. I agree that permission to copy from, or to publish from, this dissertation may be granted by the professor under whose direction it was written, or, in his absence, by the Dean of the Graduate Division when such copying or publication is solely for scholarly purposes and does not involve potential financial gain. It is understood that any copying from, or publication of, this dissertation which involves potential financial gain will not be allowed without written permission.

[redacted]

7/25/68

PARAMETRIC CONSIDERATIONS IN THE DESIGN AND PERFORMANCE OF A FLUIDIC DIRECT IMPACT MODULATOR

A THESIS

Presented to

The Faculty of the Graduate Division

by

Ronald Wayne McGregor

In Partial Fulfillment

of the Requirements for the Degree

Master of Science in Mechanical Engineering

Georgia Institute of Technology

September, 1968

PARAMETRIC CONSIDERATIONS IN THE DESIGN AND

PERFORMANCE OF A FLUIDIC DIRECT IMPACT MODULATOR

Approved:

Chairman:

Date approved by Chairman: Nov. 25, 1968

ACKNOWLEDGMENTS

I wish to thank my Thesis Advisor, Dr. P. V. Desai, for his originating the thesis topic and for his suggestions and encouragement throughout the work. Also I wish to thank the thesis committee, Dr. W. Z. Black and Dr. Steve L. Dickerson for their time and suggestions. A special note of appreciation is due Mr. Bjorn G. Bjornsen of Johnson Service Company for his assistance in providing some of the basic research literature. My appreciation is extended to Mr. W. A. Boothe of General Electric Company and to Mr. C. P. McKenzie of Martin Marietta Corporation for their ideas and suggestions. My thanks also to Mr. Cloyd Van Hook for his help in this research and to Mrs. Louise K. Barge for her kind assistance in typing the manuscript. With permission of the Graduate Division, captions of the photographs used deviate from the thesis requirements.

I am indebted to Dr. Stothe P. Kezios, Director of the School of Mechanical Engineering, for financial assistance in the form of a graduate teaching assistantship and also to LTV Aerospace Corporation for a gracuate scholarship. Furthermore I would like to acknowledge the patience and encouragement of my office mate and colleague, Allan Lindsey, who was forced to endure some of the more unpleasant acoustical characteristics of such a pneumatic investigation. I am grateful to my parents for their assistance and encouragement through these years of academic trials and guidance of the Creator, whose blessings have made my effort rewarding.

TABLE OF CONTENTS

TABLE OF CONTENTS (Cont'd)

LIST OF TABLES

LIST OF ILLUSTRATIONS

LIST OF ILLUSTRATIONS (Cont'd)

SUMMARY

The current investigation explored a new concept in fluidic amplification in the form of a direct impact modulator (DIM). This was the first known venture in constructing a variable geometry device such that a parametric study of both pressure and geometric variables could be attempted. Because of the complexities of compressible flow, and particularly due to the lack of knowledge concerning impacting pneumatic jets, a completely experimental investigation was conducted to determine the range of operation and characteristics of the DIM.

Working on the principle of impacting air jets and the modulation of the radial impact plane formed by two opposing supply jets, the DIM was known to possess high gains, particularly pressure gains, and an unusual insensitivity to change in output impedance. After studying a preliminary design, a modified nozzle assembly was constructed, tested, and evaluated. Alignment accuracy of the nozzle orifices was found to be the most influential factor affecting the performance of the device. Two constraints were imposed on the nozzle separation distances; these were: 1) the Coanda attachment phenomenon at the minimum distance and 2) instability of the jet impact region beyond the maximum distances. Primary to secondary nozzle separation was the most sensitive geometrical variable. The output pressure was fairly insensitive to changes in the output impedance. Pressure gains in the DIM were somewhat smaller than those expected. Manufacturing inaccuracies, misalignment, and boundary

layer disturbances caused by rough surfaces were cited as causes for the poor performance. Flow gain, on the other hand, was encouraging.

A new nozzle configuration based on the results of this investigation was proposed and an outline for optical alignment was suggested. Definite values for geometric and dynamic variables were found for satisfactory performance with respect to pressure gain. In general, the work was more investigatory than definitive, due to the complex, and non-linear behavior of this novel pneumatic device.

NOMENCLATURE

s	primary-secondary nozzle separation distance--inches
L	secondary nozzle separation distance--inches
psig	pressure--pounds per square inch gage
P_i	input pressure (emitter secondary)--psig
P_c	output pressure (collector secondary)--psig
P_e	emitter supply pressure (emitter primary)--psig
P_c	collector supply pressure (collector primary)--psig
P_s	nominal supply pressure level--psig
G_p	pressure gain
G_f	flow gain
Z	fluidic impedance--subscript denotes the number of valves closed
D	primary nozzle orifice diameter--inches (held constant in this research)
d	secondary nozzle orifice diameter--inches (held constant in this research)
Q	volumetric flow rate--cubic feet per minute
W_i	input mass flow rate--pounds mass per minute
W_o	output mass flow rate--pounds mass per minute
W_s	supply mass flow rate--pounds mass per minute
ρ	density
x	distance along the axis of an axisymmetric jet--inches
y	distance normal to the centerline of an axisymmetric
s_m	maximum primary to secondary separation distance--inches

CHAPTER I

INTRODUCTION

Historical Background

The impact of pheumatic jets was first studied by Edme Mariotte (1620-1684) (1). Nozzle flow and jet impact continued to be analyzed with the result of well defined theories for certain cases (2). However the complexities of compressible flow imposed some rather rigorous mathematics and undefined boundary conditions, not to mention the numerous simplifying assumptions required. As a result, empirical effort by the fluid dynamicists characterized the study of turbulent jets (3).

With the advent of pure fluid control development--the science of fluidics--in the early 1960's, the impact principle became a model for a new concept in fluid amplification. The Johnson Service Company of Milwaukee, Wisconsin, conducted a research and development program to study the feasibility of using the impact principle for fluid amplification. As a result of this research, the concept was proven and interest was immediately generated in the fluidic community.

In 1967 a direct impact modulator nozzle assembly was constructed at the Georgia Institute of Technology. The design and construction detail of the modulator were the result of a special project (4). Another nozzle set was designed and tested after a preliminary evaluation of the first nozzles. The test and evaluation of the direct impact modulator was the object of this research; this investigation

was thought to be the first attempt at constructing a direct impact modulator such that geometrical and pressure variables could be adjusted independently

Jet Theory

Submerged jets were found to be an object on intense study with regard to velocity profiles, turbulence, and potential flow regions. The ideal, turbulent, two-dimensional jet was known to expand somewhat linearly downstream (5), (6). Certain regions could be recognized such as a wedge-shaped potential core extending some 5.2 nozzle diameters downstream from the point of efflux, a divergent envelope of turbulent shear layer surrounding the potential core, and a fully developed turbulent mixing region (7). To describe the velocity profile in both the transition zone and the fully developed zone, the following equation was advanced (8).

$$\frac{V}{V_M} = \left[1 - \left(\frac{y_e}{0.265x}\right)^{\frac{7}{4}}\right]^2$$

where V_M was the centerline velocity, y_e was the effective value of y for the transition zone and the actual value of y for the fully developed zone (see Figure 1, page 3). By integration of the velocity profile, total flow and energy predictions for the jet were possible (8). Figure 1, page 3, shows a model of the two-dimension, turbulent jet expansion adapted from reference (8).

It was also known that downstream from the point where the potential core ended, the maximum velocity of the jet decreased as the

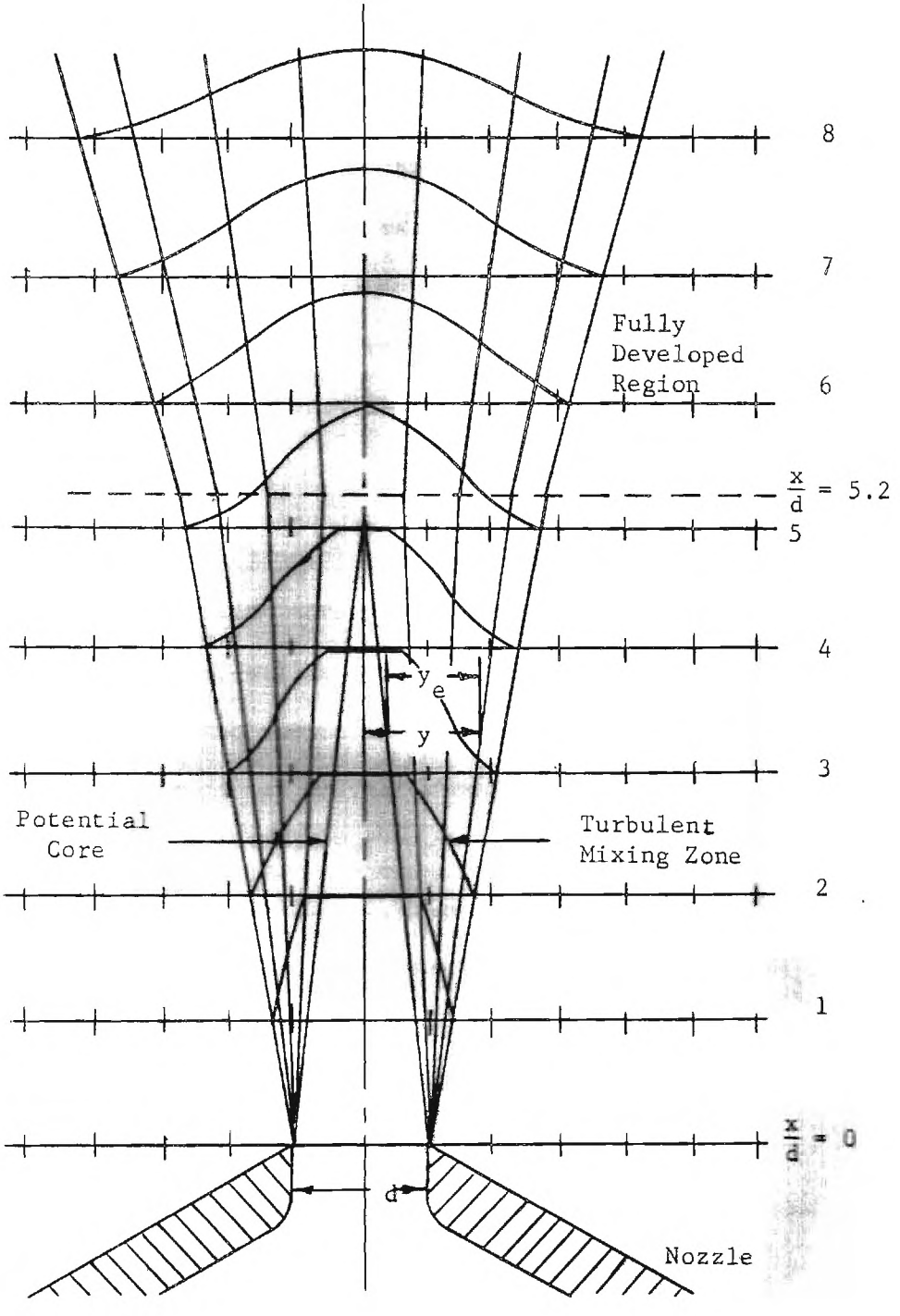

Figure 1. Velocity Profile of a Power Jet (Ref. 8)

diffusion zone expanded. This diffusion continued theoretically until the jet became infinitely large and of zero velocity, expanding to ambient conditions (9). Ambient entrainment, due to viscous effects, was also known to be a characteristic of the submerged jet. In the more realistic case of the submerged, axisymmetric turbulent jet, regions similar to those described above could be identified, however the expansion profile was probably curved outward due to edge effects and the turbulent mixing. However the ideal model was used for calculations in this research.

Principles of Operation

In comparision with stream deflection fluidic devices, the direct impact modulator utilized a new concept in the change of momentum flux to modulate the output. If two axially symmetric jets were placed in opposition to one another along their center lines, flow from the jets would impact in a radial fashion, forming an impact plane between the two jets as in Figure 2, page 5. The location of this impact region would depend upon the momentum flux difference between the jets issuing from the nozzles, the pressure gradients in the impact region, and the turbulence levels of the jets. By increasing the power of one of the jets, the radial impact region would move away from this jet toward the opposing jet. If a circular "collector" were placed concentric with the centerline in the region between the jets, the impact momentum could be recovered and thus by changing the power level of one of the jets, the impact region would move relative to the collector, and a "modulated" output could be obtained. Amplification implies a magnification of the output due to an input whereas modulation connotes

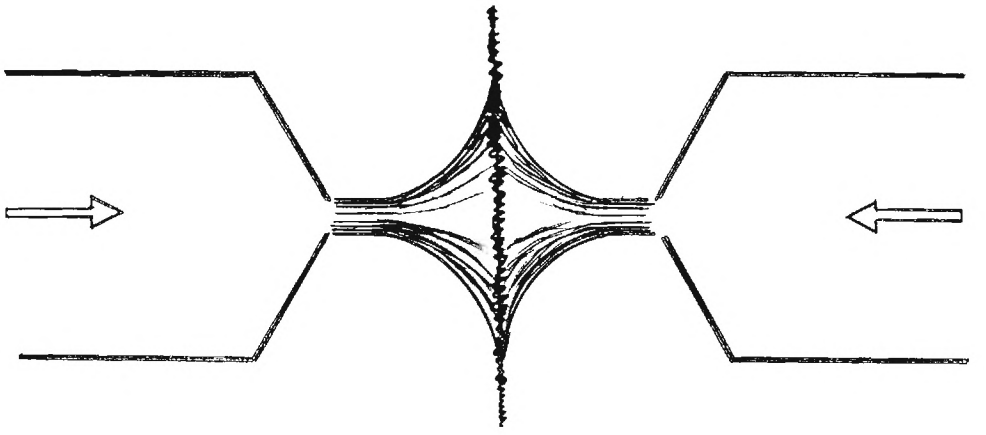

Figure 2. Radial Impact Plane Between Two Jets

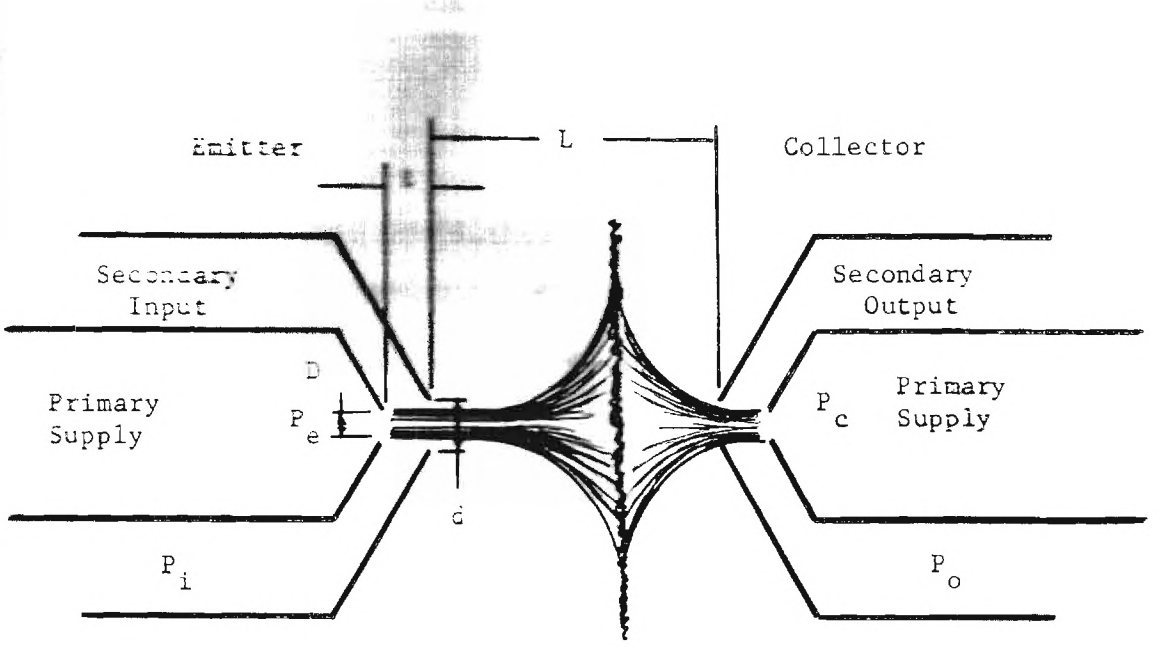

Figure 3. The Direct Impact Modulator Configuration

only a change in the intensity of the output without regard to scaling direction. Accordingly the DIM was properly termed a modulator or amplifier.

As a further consideration, if both jets were maintained at constant power levels, and an input were imposed through an annulus surrounding one of the jets, this input would "focus" the supply jet, moving the impact region, and the output could be collected around the opposing jet through a similar annulus. Thus a symmetrical configuration could be constructed as shown in Figure 3, page 5. With reference to Figure 3, the input side will be referred to as the emitter, with the internal supply nozzle known as the primary supply, and the input. Similarly the output side will be referred to as the collector, with primary supply and secondary output.

Significant Variables of Operation

The often used analogies between fluidic and electronic circuitry were obtained by comparing mass flow rate with current and pressure with potential. Fluidic impedance and power were also known to be analogous to their electrical counterparts.

Peculiar to the direct impact modulator were the variables of emitter supply pressure, P_e, emitter input pressure, p_i, collector supply pressure, P_c, and collector output pressure, P_o. Flow rate variables consisted of supply mass flow rate, W_s, emitter input mass flow rate, W_i, and collector output mass flow rate, W_o. With regard to flow rate when referring to a compressible fluid such as air, volume flow rate was inconclusive unless the corresponding pressure and temperature were specified, in which case, the ideal gas law could be

applied for an approximation to mass flow rate. Pressure gain, the ratio of collector output pressure to emitter input pressure, and flow gain, the ratio of collector output mass flow rate to emitter input mass flow rate, were also significant considerations in the design of the modulator. Geometric variables consisted of primary to secondary separation distance, L, secondary nozzle separation distance, L, and primary and secondary orifice diameters, D and d, respectively. The foregoing variables are identified in Figure 3, page 5; in this investigation, orifice diameters remained constant.

The purpose of the current research was to evaluate the effect of the previously mentioned variables on the testing of a set of nozzles for the direct impact modulator. Consequently the variables which most significantly affected the performance of the direct impact modulator were to be identified and guidelines were to be established for the construction of the modulator. This research was unique in the respect that it was the first known attempt at making a nozzle set which was variable such that a wide spectrum of tests could be conducted.

General Characteristics of Operation

The direct impact modulator, hereafter referred to as the DIM, was known to possess the quality of high pressure and flow gain, being an order of magnitude higher than the gain of a stream deflection amplifier (10). The modulator also offered the advantage of extremely high input impedance, dependent primarily upon the supply pressure level, which was required for increased sensitivity (11). High input impedance was possible due to the large negative pressure at small flow rates, caused by "aspiration" in the emitter nozzle during certain modes of

operation. Aspiration was the entrainment of ambient fluid due to the presence of a high power jet and the associated pressure drop caused by this entrainment. The amount of aspiration was dependent upon the power level of the supply jet and upon the primary to secondary separation level of the supply jet and upon the primary to secondary separation distance, ℓ , as evidenced in Figure 18 and 19, pages 53 and 54 of Appendix A. Because of this "ejector" characteristic of the DIM, negative and positive gains were possible. Negative gains occurred when the impact region was located somewhere outside the collector nozzle thus increasing the input decreased the output momentarily. Positively gains were more reasonable and characteristic of the DIM were obtained when the impact region was located at the face of the collector nozzle. In this case, increasing the input produced a corresponding increase in output. Only positive gains were of interest in this investigation.

The capability of adjusting the modulator to suit the load was a distinctive feature of the direct impact principle. Unlike a stream deflection amplifier which must be uniquely matched for a certain load, the impact modulator could be adjusted to a wide variety of output impedance merely by increasing the supply power. Besides the foregoing advantages, the DIM offered the advantages common to fluid amplifiers of insensistivity to electromagnetic radiation, vibration, or other adverse environments, a wide operating temperature range, adaptability to any fluid, no moving parts, and high reliability.

Unfortunately, the DIM, like most fluidic amplifiers, was known to be a high power consumption device; the supply jets

operated continuously regardless of the output. Other disadvantages included a relatively low signal to noise ratio, which should improve with advancing technology, critical alignment accuracy, and instability of the impact region. With the nozzle set used in this research, size would be a definite disadvantage, but smaller sizes could be possible as demonstrated by a plastic nozzle assembly designed by the Johnson Service Company, which was approximately one-half inch in diameter and one and one-half inches long (12).

The DIM could be used whenever a high gain amplifier, capable of being matched to a variety of loads, was required. Some applications could include an active element in a fluidic analog computer (11), fluidic controller (13), fluidic summers (14), or a cascaded unit in a power amplification module.

CHAPTER II

THE MODULATOR AND TEST EQUIPMENT

Modulator Design

The first DIM nozzle set, Configuration A, was a geometrically similar adaptation from a previous design (15). Sharp edges were faired to decrease the chance of separation, and to generate a thinner boundary layer. The primary and secondary nozzles were constructed of brass and were threaded for mating. Register marks every one-quarter revolution provided repeatable primary to secondary separation. The secondary nozzle was fitted with a vertical tube for secondary input or output and a small capillary tube in the vertical tube provided a pressure tap. The primary inputs were supplied directly to the horizontal nozzle. Figure 4, page 11, shows the mounted nozzle assembly and Figure 2, page 59, of Appendix B shows nozzle details.

Both the emitter and collector nozzle assemblies were mounted on a one-dimensional traversing mechanism to provide colliner separation of the compound nozzles as shown in Figure 24, page 62, of Appendix B. A scale and pointer arrangement on the base of the traverse indicated the nozzle separation distance, L. All orifices as dimensioned in Figure 21, page 59, were through drilled after the compound nozzles were mounted in the traversing mechanism to assure concentricity and axial alignment. It should be mentioned at this point that alignment was suspected to be very critical in the performance of the DIM.

Page missing from thesis

This suspicion was corrobrated by this author, in the literature (3) and by personal contacts at the Martin Marietta Company and at General Electric. However, the best possible accuracy was sought with the available equipment, using the above procedure.

The nozzle set finally used, configuration D, shown in Figure 5, page 13, was constructed of Plexiglas. To circumvent the alignment problem due to threads in Configuration A, the second nozzle set utilized a sliding primary nozzle with an "O" ring seal. This arrangement provided a positive alignment since orifices were drilled with nozzles in contact. Dial indicators were used to set the primary-secondary separation distance, using the bottomed position as a reference. The new design incorporated beveled nozzle faces to obviate the attachment experienced in Configuration A. Plexiglas was chosen for the nozzles because of availability and ease in machining; basic dimensions of the nozzle remained the same. Two other nozzle designs were proposed, but were revised to the final configuration. The nozzle details are shown in Figure 22, page 60, of Appendix B.

Test Panel

A test panel was designed and constructed to provide flow and pressure measurements and loading capabilities; the schematic is shown in Figure 25, page 63, of Appendix B. A clean, dry twenty psig shop air source was provided to the panel through filters, a regulator, and a stagnation tank. Laminar flow elements and inclined manometers provided supply and output flow rates, with a small rotameter used to register input flow rate. Bourdon-type gages were used to measure stagnation tank pressures and supply pressures, with oil and mercury

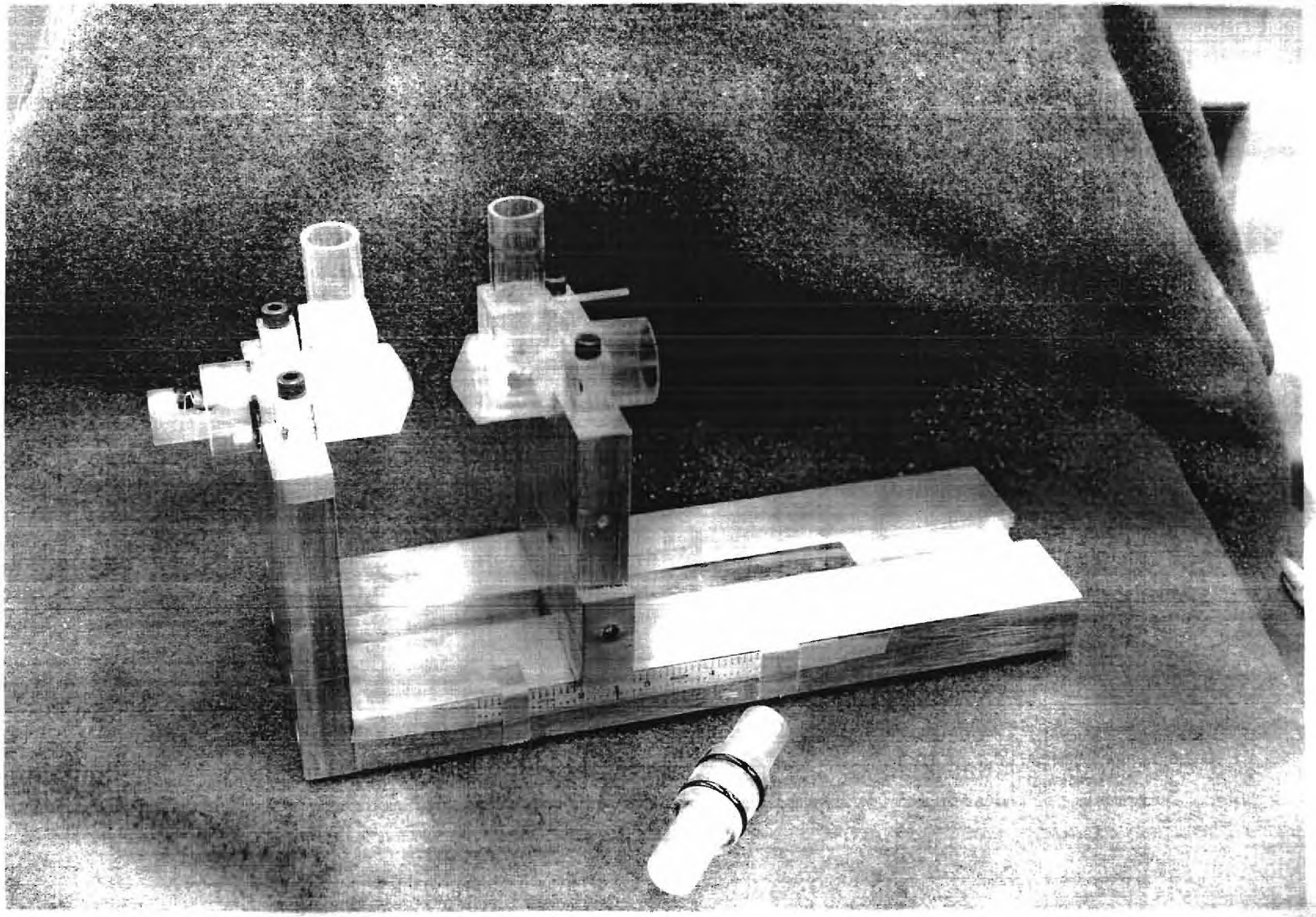

FIGURE 5 CONFIGURATION D NOZZLE ASSEMBLY

manometers being used for input and output pressures respectively. A small oil manometer was also used in the output line to establish initial conditions. Supply flows were controlled by a regulating stem valve while input power was monitored with a very precise needle valve. An output impedance manifold was constructed with four toggle valves and orifices, in parallel. This arrangement provided the capability of increasing the load in a stepwise and repeatable fashion from approximately no load up to infinite load. Additional load was available with the attachment of four capillary tubes to the orifices should such be required. Figures 6 and 7, pages 15 and 16, show the front view and side elevation of the test panel respectively.

Sizing Criteria

The modulator dimensions were scaled up from the original design (15) because of manufacturing limitations. However these sizes were large in comparison with those found in the literature (3)(13). Twenty psig was chosen as the stagnation tank supply pressure limit since this was the maximum pressure for linearity of the laminar flow element (16). Also the chosen supply pressure represented a nominal operating pressure of commercially available fluidic components (13). Bourdon gages were selected such that their full scale reading was approximately twice the expected pressure. The collector supply gage was selected with a larger range, however, due to the oscillations which were known to exist during some phases of operation. This research was to be limited to the subsonic flow regime of air to constrain an already complex analysis and to investigate the DIM in a low power level mode of operation. Assuming that the nozzle exit pressure was approximately atmospheric

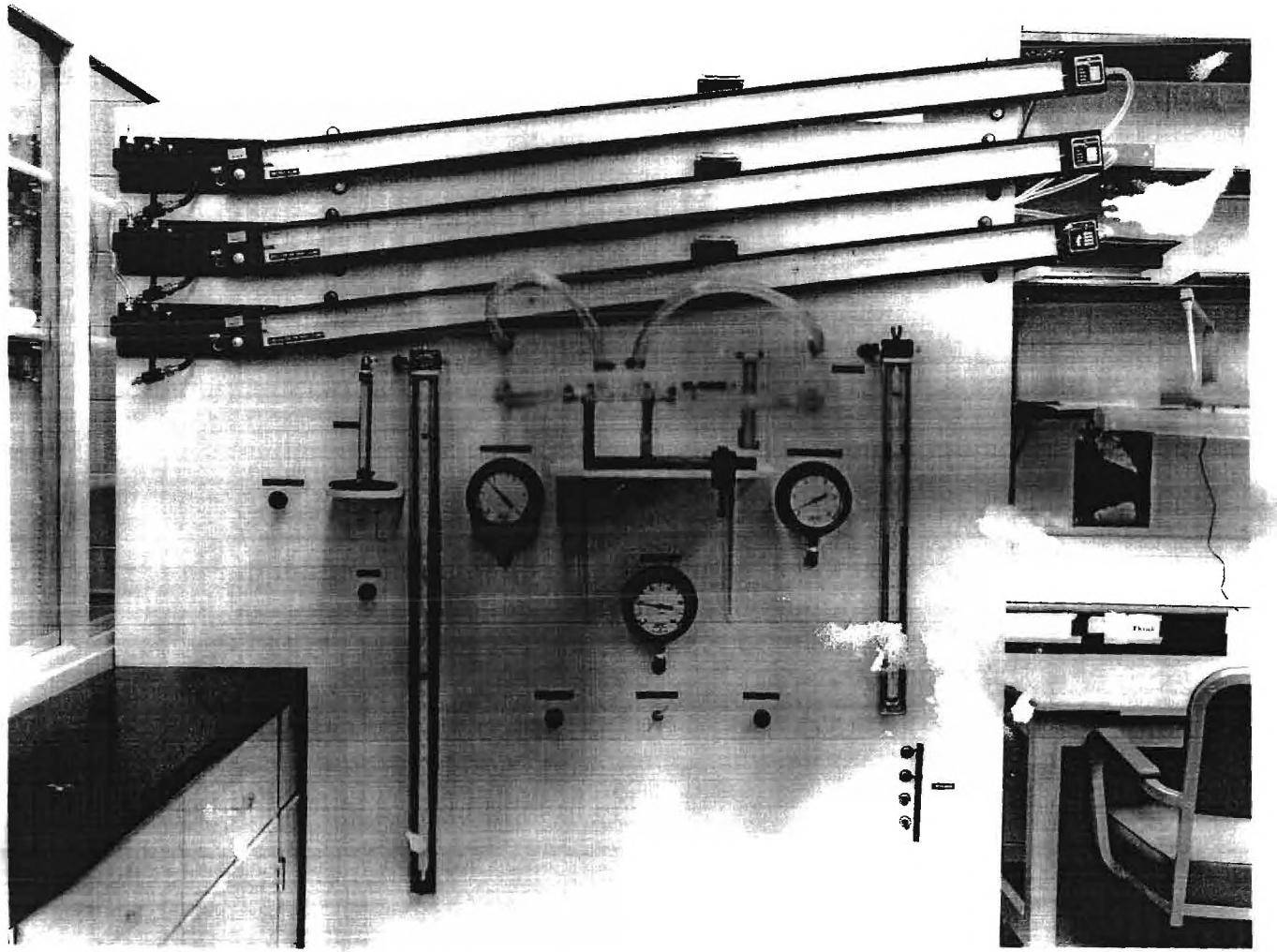

FIGURE 6 FRONTAL VIEW OF TEST PANEL

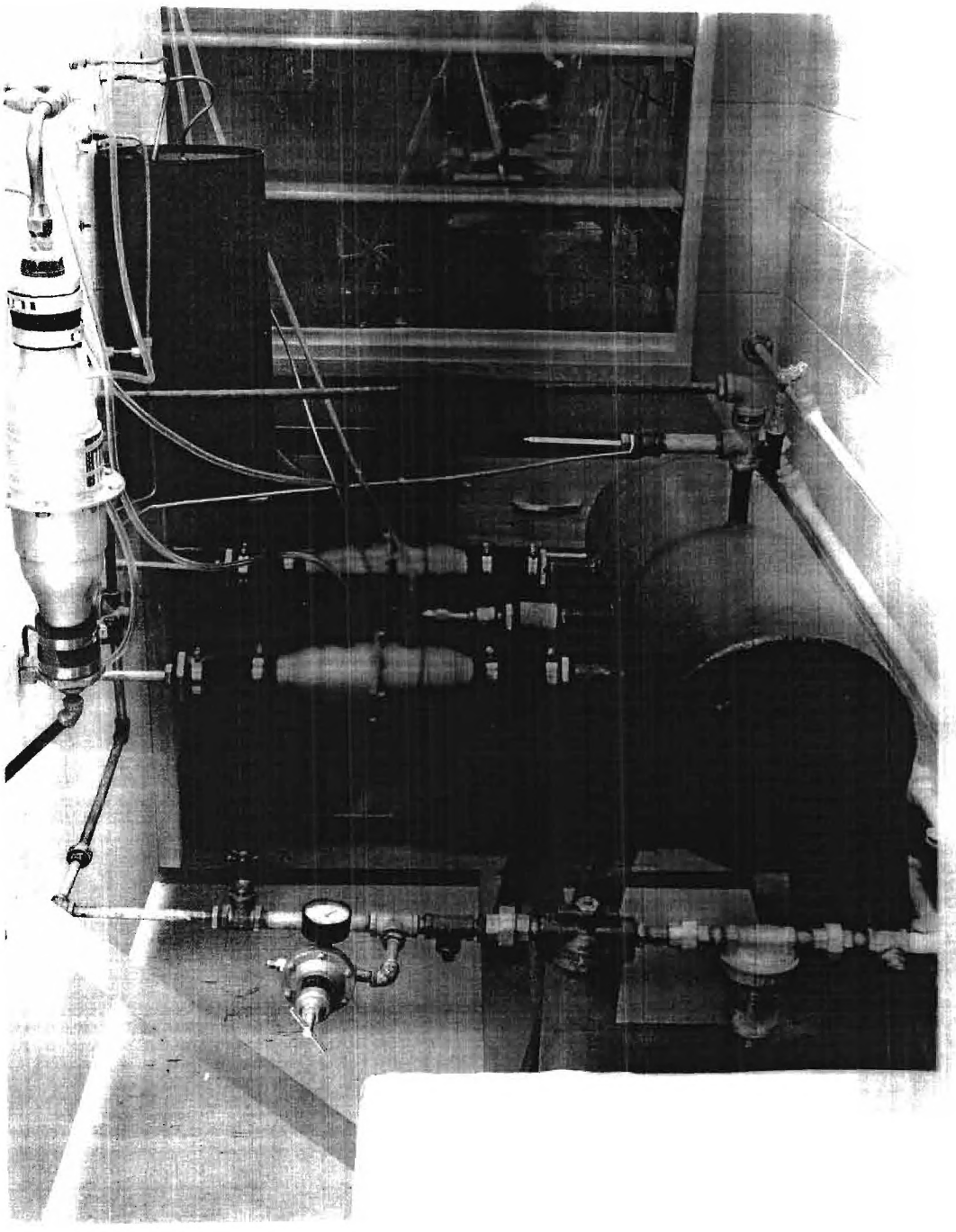

FIGURE 7 SIDE ELEVATION OF TEST PANEL

and that the pressure read as supply was approximately the stagnation pressure, 13 psig was calculated as the maximum pressure for the maintainence of subsonic flow (see Appendix A page 50). To compensate for assumptions, 12 psig was selected as the maximum supply pressure and a 24 inch mercury manometer was then employed for the ouput pressure measurement. The laminar flow elements were chosen for their ability to measure very low flow rates and for their linear response. Line sizes were selected for ease of assembly,compatibility with valves, and minimization of losses. The test panel was designed with external fittings affixed to the panel front for the attachment of Tygon tubing which supplied the modulator. This configuration was chosen so the panel could serve as a universal test stand for further fluidic investigations and also to provide mobility for the traversing mechanism.

CHAPTER III

EXPERIMENTAL PROCEDURE

Initial Investigations--Configuration A

An investigation of the brass nozzles, Configuration A, revealed that they were defective. First a series of tests were conducted at varying pressures and separation distances with nozzles in the impact configuration, but adverse instability and non-repeatability indicated a deficiency in the nozzle assembly. Next a test of nozzle characteristics was performed on each nozzle set individually by varying the supply pressure and noting the secondary plenum pressure as the primary to secondary separation was changed by rotating the internal nozzle. During this test, no flow was permitted through the secondary plenum. Results of the tests proved the nozzle sets to be dissimilar, one set appearing to possess an irregularity which repeated with every revolution of the nozzle. Based on this fact, the orifice of the primary nozzle was observed to be misaligned with the secondary nozzle orifice, aligning itself at only one point on every revolution. This inconsistency was due to the use of screw threads as a means of centering the orifices. A new primary nozzle was constructed with carefully drilled orifices in an attempt to rectify the error, but the effort was futile. Configuration D nozzles were then constructed and prepared for evaluation.

Preliminary Survey and Constraints--Configuration D

The first test conducted was to determine the maximum primary-

secondary nozzle separation distance, ℓ, for which aspiration from the secondary nozzle plenum was still possible. This test established a constraint, since a positive pressure in the plenum would mean that the primary jet was expanding within the plenum, thus defeating the purpose of the modulator. Of equal importance, this test served as a comparison of the characteristics of the emitter and collector nozzle assemblies, similarity of which was desirable in this parametric study. To perform this test, the primary nozzle was supplied from the test stand with pressures of six, eight, ten and twelve psig for each chosen separation distance, ℓ, and pressures were measured in the secondary plenum when there was no flow into the secondary. Nozzle characteristics appear in Appendix A as Figures 18 and 19, pages 53 and 54.

Several constraints were known to exist such that a bounded test spectrum could be prescribed prior to testing. The first constraint, and one previously mentioned, was the subsonic flow requirement which limited the supply pressure to something less than 13 psig. Secondly, because of the attachment phenomenon, close nozzle separation distances, L, were excluded from the spectrum. Instability of the impact region at these small distances, as witnessed by Misevich, corroborated the exclusion (17). This qualitative separation judgement acted to establish proper limits on the investigation rather than to prescribe distances initially. Thirdly, there was a certain maximum secondary nozzle separation distance, L, beyond which the modulator was ineffective. This constraint was due to the rupturing of the potential cores by the associated turbulence of the impacting supply jets and was known to be about six nozzle diameters (3). Finally using the model of jet ex-

pansion previously described, a maximum primary to secondary separation distance, λ, could be calculated such as to prevent a positive pressure in the secondary plenum as mentioned above.

Initial Conditions

The prescription of an initial base point was very important to the operation of any device characterized by numerous variables. The DIM, as an amplifier, should display a zero output for zero input. Pursuant to this objective, after geometric and output impedance adjustments, the emitter supply pressure was set at a prescribed level, producing aspiration in the secondary plenum. The input flow was then adjusted until the input plenum pressure reached a reference value--for this case, atmospheric. The collector pressure was then increased until atmospheric pressure was also measured in the output plenum. At this initial point, the jet impact region was established partially inside and on the face of the collector nozzle assembly, the location being characterized by a crackling, sputtering sound. This position was verified experimentally by noting the depression on one's finger when held beneath the collector nozzle. As the distance between nozzles was traversed, only at this one place was the impact region evident. The initial point was also rationalized based on the amplification effect desired, i.e., if the impact region were somewhere between the emitter and collector, this position would represent a "dead band" in the input-output characteristics. Starting from this operating point, the DIM functioned as an electrical amplifier, with output power increasing as input power was supplied. Other initial conditions could be imposed, but a common base point must be decided upon; the above

mentioned procedure was similar to the one used by Bjornsen (12). The most important requirements for any base point were that the conditions be readily reproducible and repeatable for any device. The initial conditions for the DIM had to be reset each time the output impedance, the supply pressure, or geometric variables were adjusted. Incremental inputs were repeated for each supply pressure and geometric combinations and ouput flow and pressure were recorded.

The Test Spectrum

Utilizing the previously mentioned constraints and results from the preliminary survey, a logical testing sequence was proposed. The test was composed of four blocks, each of which became progressively more discrete. The first three segments were conducted using a constant output impedance. Block I consisted of pressure and geometric variables as shown in Table 1, page 22, 23. After setting initial conditions, one input pressure was applied, and the corresponding output was noted. Results of Block I described the operating combinations for which the initial conditions could be attained, and for which the output was relatively stable.

Using the most favorable results of the previous test, a new test plan, Block II, was devised as shown in Table 2, pages 24-26. Several input pressures were applied, and outputs were compared. The initial conditions were impossible to set at ten psig due to instability of the jet impact region. Thus to provide additional data, a supply pressure of four psig was selected. Higher resolution in the prescription of geometric variables was the ojbect of Block II.

Table 1. Block I Test Parameters and Results
(P_i = 6 inches of oil)

ℓ In.	L In.	P_s-psig	P_o In./Hg.	Remarks
0.025	0.3	6	-	Initial Conditions Unattained
0.025	0.3	8	-	Initial Conditions Unattained
0.025	0.3	10	-	Initial Conditions Unattained
0.025	0.4	6	-	Initial Conditions Unattained
0.025	0.4	8	3.0	Sensitive
0.025	0.4	10	1.5	Sensitive
0.025	0.5	6	-	Initial Conditions Unattained
0.025	0.5	8	-	Initial Conditions Unattained
0.025	0.5	10	0.1	Sensitive
0.025	0.6	6	-	Initial Conditions Unattained
0.025	0.6	8	0	
0.025	0.6	10	0	
0.025	0.7	6	-	Initial Conditions Unattained
0.025	0.7	8	-	Initial Conditions Unattained
0.025	0.7	10	-	Initial Conditions Unattained
0.050	0.3	6	1.0	
0.050	0.3	8	1.5	Unsteady
0.050	0.3	10	0.8	
0.050	0.4	6	0.8	
0.050	0.4	8	1.0	Unsteady
0.050	0.4	10	0.2	
0.050	0.5	6	0.6	
0.050	0.5	8	0.2	Unsteady
0.050	0.5	10	0.05	
0.050	0.6	6	0.2	
0.050	0.6	8	0.1	
0.050	0.6	10	0.02	
0.050	0.7	6	0	
0.050	0.7	8	0	
0.050	0.7	10	0	
0.075	0.3	6	0.8	
0.075	0.3	8	1.5	Unsteady
0.075	0.3	10	0.2	
0.075	0.4	6	0.5	
0.075	0.4	8	-	
0.075	0.4	10	0	Sensitive
0.075	0.5	6	0.4	
0.075	0.5	8	0	
0.075	0.5	10	0	
0.075	0.6	6	0.5	

Table 1. Block I Test Parameters and Results
(P_i = 6 inches of oil)
(continued)

ℓ In.	L In.	P_s-psig	P_o In./Hg	Remarks
0.075	0.6	8	0	
0.075	0.6	10	0	
0.075	0.7	6	0	
0.075	0.7	8	0	
0.075	0.7	10	0	

Table 2. Block II Test Parameters and Results

P_s psig	P_e psig	P_c psig	P_i in/oil	P_o In./Hg.	Remarks
ℓ = 0.06 L = 0.35					
4	3.9	3.2	1	0.05	
4	3.9	3.2	3	0.2	
6	5.8	4.5	1	0.02	
6	5.8	4.5	3	0.5	Unstable
8	7.6	6.3	1	0	
8	7.6	6.3	3	0.01	
ℓ = 0.06 L = 0.45					
4	3.95	2.6	1	0.01	
4	3.95	2.6	3	0.17	
6	5.9	3.75	1	0.01	
6	5.9	3.75	3	0.15	
8	7.88	5.2	1	0	
8	7.88	5.2	3	0	
ℓ = 0.06 L = 0.55					
4	3.95	2.45	1	0	
4	3.95	2.45	3	0	
6	5.75	3.2	1	0.02	
6	5.75	3.2	3	0.07	
8	7.8	4.2	1	0	Unstable
8	7.8	4.2	3	0	
ℓ = 0.045 L = 0.35					
4	3.9	3.25	1	0.3	
4	3.9	3.25	3	0.65	
6	5.9	5.0	1	0	
6	5.9	5.0	3	0.35	
8	7.6	6.2	1	0	Unstable
8	7.6	6.2	3	0.2	

Table 2. Block II Test Parameters and Results (continued)

P_s psig	P_e psig	P_c psig	P_i in/oil	P_o In./Hg.	Remarks
ℓ = 0.045 L = 0.45					
4	3.9	2.8	1	0.05	
4	3.9	2.8	3	0.2	
6	5.8	4.0	1	0.05	
6	5.8	4.0	3	0.3	
8	7.75	5.3	1	0	Unstable
ℓ = 0.045 L = 0.55					
4	3.9	2.4	1	0	
4	3.9	2.4	3	0.1	
6	5.85	3.5	1	0	
6	5.87	3.5	3	0	
8	7.75	3.5	1	0	
8	7.75	3.5	3	0	
ℓ = 0.030 L = 0.35					
4	-	-	-	-	Initial Condition
4	-	-	-	-	Unattained
6	5.75	4.1	1	0.1	
6	5.75	4.1	3	0.35	
8	-	-	-	-	Initial Condition
8	-	-	-	-	Unattained
ℓ = 0.030 L = 0.45					
4	4.0	3.0	1	0.1	
4	4.0	3.0	3	0.4	
6	5.8	4.2	1	0.01	
6	5.8	4.2	3	0.3	
8	7.6	5.3	1	0	Unstable
8	7.6	5.3	3	0	

Table 2. Block II Test Parameters and Results
(continued)

P_s psig	P_e psig	P_c psig	P_i in/oil	P_o In./Hg.	Remarks
ℓ = 0,030 L = 0.55					
4	3.9	2.5	1	0.01	
4	3.9	2.5	3	0.15	
6	5.8	3.5	1	0	
6	5.8	3.5	3	0.15	
8	7.8	4.4	1	0	Unstable
8	7.8	4.4	3	0	

Block III was designed to capitalize upon the best results of Block II with respect to output pressure levels. This third test was conducted with the parameters shown in Table 3, page 28. As shown in Table 3, the eight psig supply pressure yielded low output pressures and was unstable. Accordingly this supply pressure was omitted from the test spectrum in favor of the four and six psig. The Block IV test regime was an analysis of five of the best combinations of geometries and supply pressures, with respect to pressure gains. In this test, the output impedance was varied from practically zero to infinity (output port completely blocked), and a variety of input pressures were applied. Table 4, page 31, shows the optimum combintaion of operating points, and the pressure gains at each impedance; Table 5, page 32, shows the flow gains for each operating point. By organizing the foregoing tests, inconclusive data were restrained to a minimum and the test program in general was more directional. Data used in compiling the results for Block IV may be found in Appendix C, Tables 6-10, pages 65-69.

Table 3. Block III Summary of Test Parameters and Output Pressures (In Inches of Mercury for P_i = 3 Inches of Oil)

Separation Distances-In. \ Nominal Supply Pressures	4	6	8
ℓ = 0.045			
L = 0.30	0.4	0.4	0.1
L = 0.35	0.65	0.35	0.1
L = 0.40	0.35	0.25	-
ℓ = 0.050			
L = 0.30	0.3	0.3	0.1
L = 0.35	0.5	0.5	0.4
L = 0.40	0.35	0.25	0.2
ℓ = 0.055			
L = 0.30	0.3	0.3	0.2
L = 0.35	0.4	0.3	0.15
L = 0.40	0.3	0.2	0

CHAPTER IV

DISCUSSION OF RESULTS

Preliminary Survey

The preliminary test on the Configuration D nozzles demonstrated that the characteristics of each were similar although not identical. Slight variations in geometry due to manufacturing techniques were thought to be the cause of the difference shown in Appendix A, Figures 18 and 19, pages 53 and 54. The maximum primary-secondary separation distance, ℓ, for aspiration to occur was shown to be about 0.06 inches. However, using the theoretical model of a jet, Figure 1, page 3, a primary-secondary separation distance of 0.0116 inches was calculated. This difference was the result of using an idealized model irrespective of pressure effects and geometrical aberations. Calculations are included in Appendix A.

Pressure and Flow

A general comment would be in order concerning gains. Pressure gains could be described by maintaining a constant output impedance, inputting a signal pressure and comparing the output pressure with the input pressure. As another approach, the output impedance could be varied to provide a constant mass flow rate at any input and then the output pressure could be monitored. The latter approach would be difficult because in compressible flow, the pressure affects the density which in turn affects the mass flow rate in a non-linear fashion. Thus

a trial and error approach of setting the impedance would be employed. The current research used the former method of prescribing pressure gains. Similarly for flow gains, the output impedance could be set, the input flow supplied, and the output flow measured. Alternatively, the impedance could be adjusted for a constant output pressure at each output flow reading and the results compared. Since the former method allowed ease in data acquisition for both flow and pressure and since a continuously variable output impedance was not available, the impedance was held constant during a run. Ostensibly, optimum flow and pressure gains would not occur at the same operating point.

As mentioned earlier, high pressure and flow gains were known to be characteristics of the DIM (10), (11), and (12). However, the results of this research were disappointing with respect to pressure gains. The DIM should have exhibited pressure gains of an order of magnitude greater than stream deflection amplifier gains of five to seven (14). Again slight misalignment and manufacturing inaccuracy were responsible for this incongruency. Table 4, page 31, summarizes the pressure gains found at the various conditions. Note that maximum pressure gains occurred generally at some median value of input pressure, and decayed for input pressures above or below that level. Ironically, flow gains were somewhat more spectacular than pressure gains. There was a distinction made in the case of flow gains, however, for at the initial condition, an input flow was being supplied to maintain atmospheric pressure in the secondary plenum. Flow gains also demonstrated the behavior of pressure gains in that there was a peak gain at one operating point, with decay on either side for most cases.

Table 4. Block IV Pressure Gains

P_i Impedance in of oil	Z_o	Z_1	Z_2	Z_3	Z_4
P_s = 6 psig	ℓ = 0.045	L = 0.30	Runs 1-5		
2	1.65	1.65	1.65	2.48	2.47
6	2.47	2.19	2.19	2.20	2.19
10	2.38	2.23	1.90	1.98	1.97
P_s = 4 psig	ℓ = 0.045	L = 0.35	Runs 6-10		
2	3.29	3.30	4.13	3.30	3.29
6	2.20	2.39	1.93	2.47	2.33
10	1.81	2.06	1.81	1.98	2.06
P_s = 6 psig	ℓ = 0.050	L = 0.35	Runs 11-15		
2	0.50	2.47	0.76	2.47	2.47
6	1.51	2.88	1.51	2.89	2.88
10	2.06	2.88	1.73	2.80	2.80
P_s = 4 psig	ℓ = 0.055	L = 0.35	Runs 16-20		
2	2.47	2.49	1.65	1.65	1.65
6	2.61	2.19	2.34	2.06	1.84
10	2.06	1.90	2.06	2.16	1.90
P_s = 4 psig	ℓ = 0.050	L = 0.40	Runs 21-25		
2	1.03	1.23	1.25	1.65	2.48
6	1.65	1.65	1.79	2.06	2.19
10	1.65	1.73	1.73	2.01	1.90

Table 5. Block IV Flow Gains
(Note: No Flow at Z_4)

Impedance in P_i of oil	Z_o	Z_1	Z_2	Z_3
P_s = 6 psig	ℓ = 0.045	L = 0.30	Runs 1-5	
2	4.00	2.22	2.22	1.54
6	5.80	5.30	2.95	1.50
10	6.30	4.70	3.40	2.06
P_s = 4 psig	ℓ = 0.045	L = 0.35	Runs 6-10	
2	10.04	5.70	4.57	2.31
6	8.00	5.20	4.27	1.82
10	7.30	4.07	3.47	2.14
P_s = 6 psig	ℓ = 0.050	L = 0.35	Runs 11-15	
2	1.54	5.22	1.08	2.50
6	4.20	6.30	3.37	2.57
10	7.27	5.90	3.40	2.54
P_s = 4 psig	ℓ = 0.055	L = 0.35	Runs 16-20	
2	4.30	3.00	2.14	1.08
6	5.70	4.37	3.36	1.72
10	5.00	4.21	3.43	1.48
P_s = 4 psig	ℓ = 0.050	L = 0.40	Runs 21-25	
2	2.50	2.14	1.43	1.54
6	5.30	3.36	2.91	1.50
10	5.50	3.79	3.00	1.53

Effect of Geometrical and Pressure Variables

Secondary nozzle separation distance was found to be bounded by two extremes--a minimum distance at which the attachment phenomenon affected the stability of the impact region and a maximum distance at which the potential core of the emitter supply jet was disrupted and stability was impossible. Tables 6-10, pages 65-69 of Appendix C expressed the best results for geometry as found in Block IV. A distance of 0.35 inches provided the best performance for both supply pressures as demonstrated by Figures 8-12, pages 34-38.

Primary-secondary separation distance, ℓ, was found to be highly critical. A deviation of 0.005 inches, centered around 0.050 inches proved to be the most acceptable performance range. It appeared that boundary layer effects and the "effective" collector plenum orifice, i.e., the annulus formed between the primary and secondary nozzles, provided an output pressure for peak gains in the region mentioned above. A separation of 0.045 inches provided the best performance as illustrated in Figures 8, 9, 10, 11, and 12.

A comment would be in order concerning the L/ℓ ratio. Although the ratio was used as a parameter in this study, care should be exercised in its application. Because of the DIM's operating characteristics, L was limited to a small range for best performance as was ℓ, thus a discrete number of choices of these parameters were available for the best L/ℓ ratio. The ratio was not continuous and one of the separation distances must be prescribed before the other could be selected. In this study, an ℓ = 0.045 and an L = 0.35 inches gave the best results as far as pressure gains were concerned. Figure 13, page 40, shows the difference

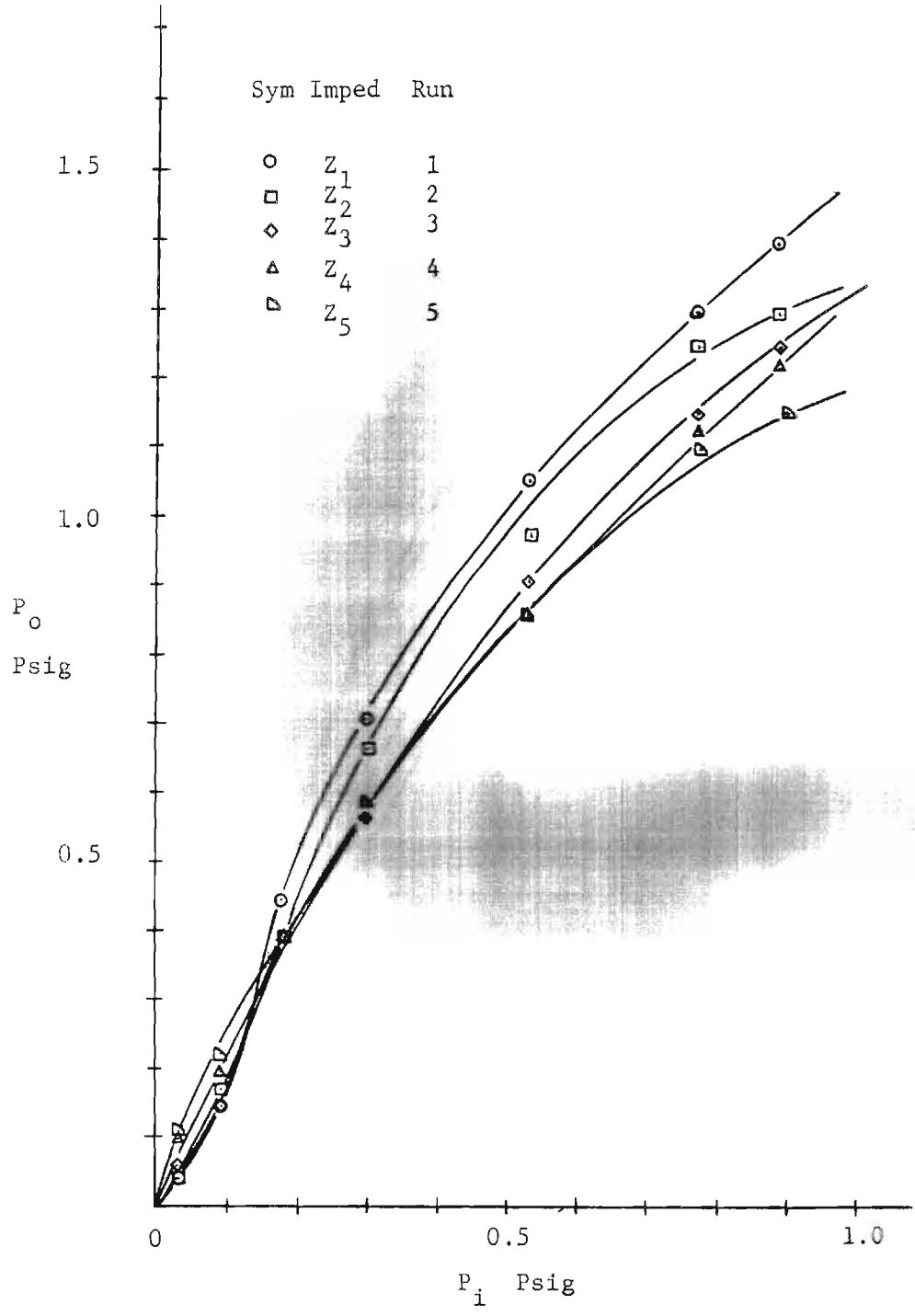

Figure 8. Output Pressure VS. Input Pressure for $L/\ell = 6.67$, $P_s = 6$ psig

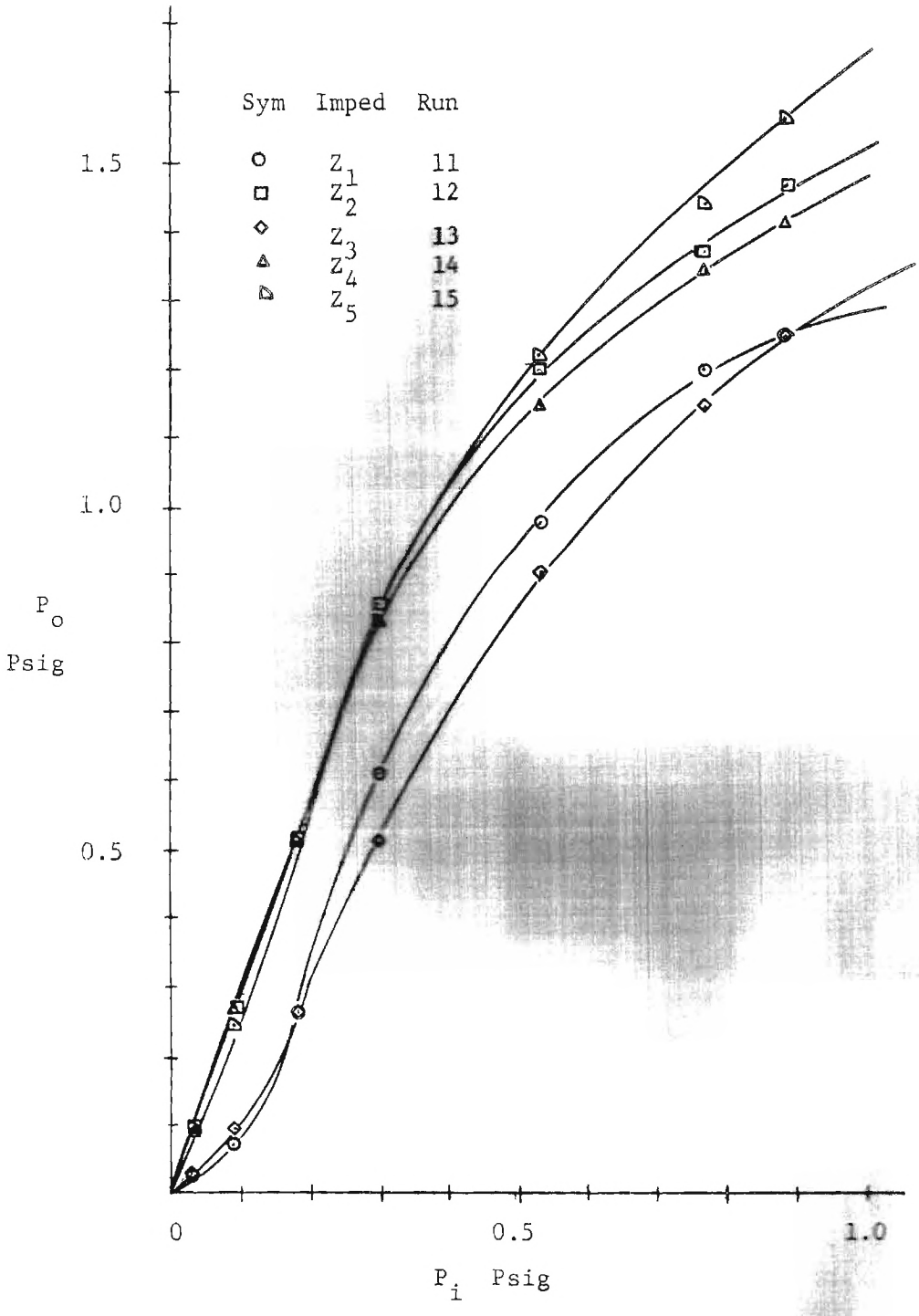

Figure 9. Output Pressure VS Input Pressure for $L/\ell = 7.00$, $P_s = 6$ psig

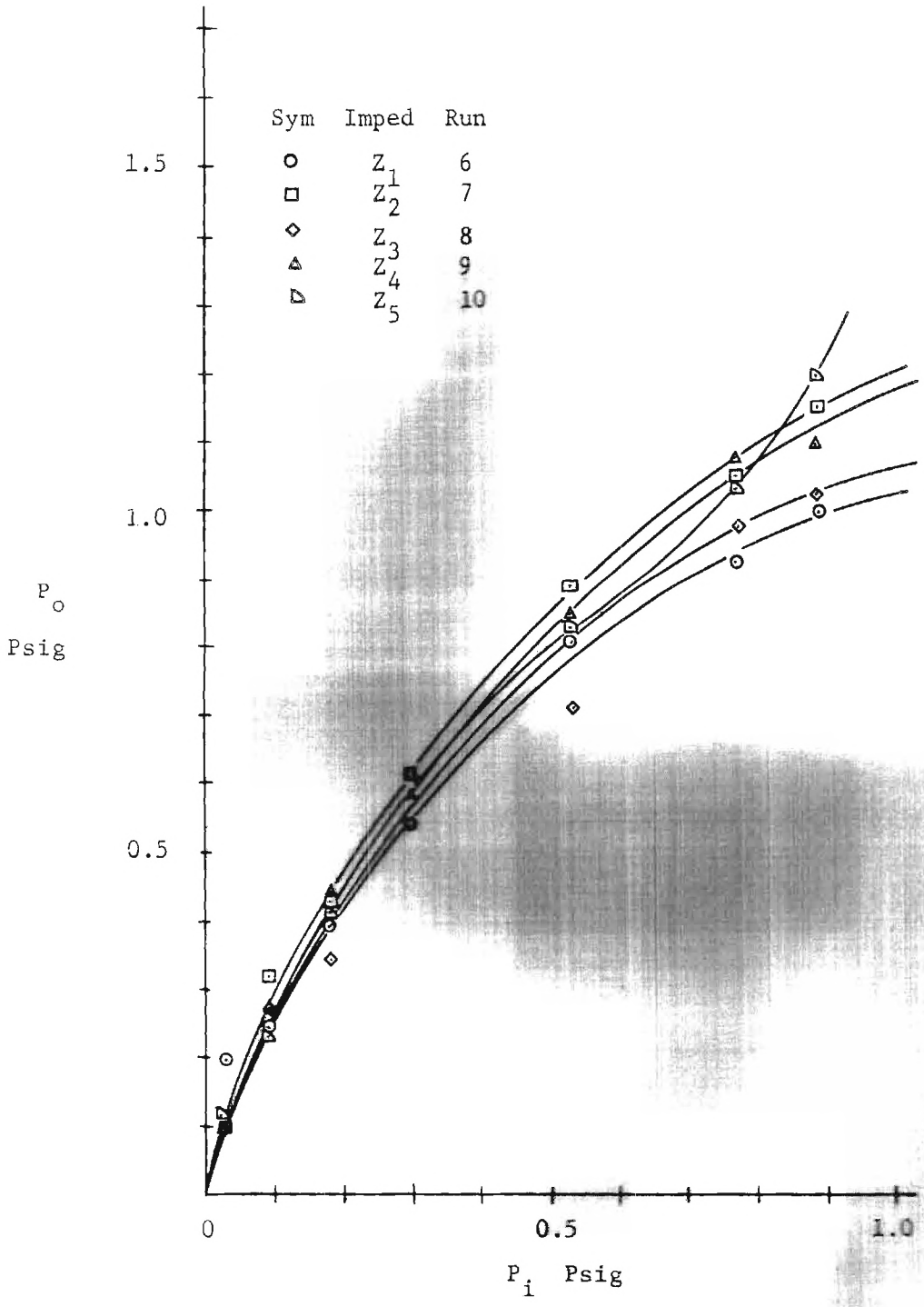

Figure 10. Output Pressure VS Input Pressure for $L/\ell = 7.77$, $P_s = 4$ psig

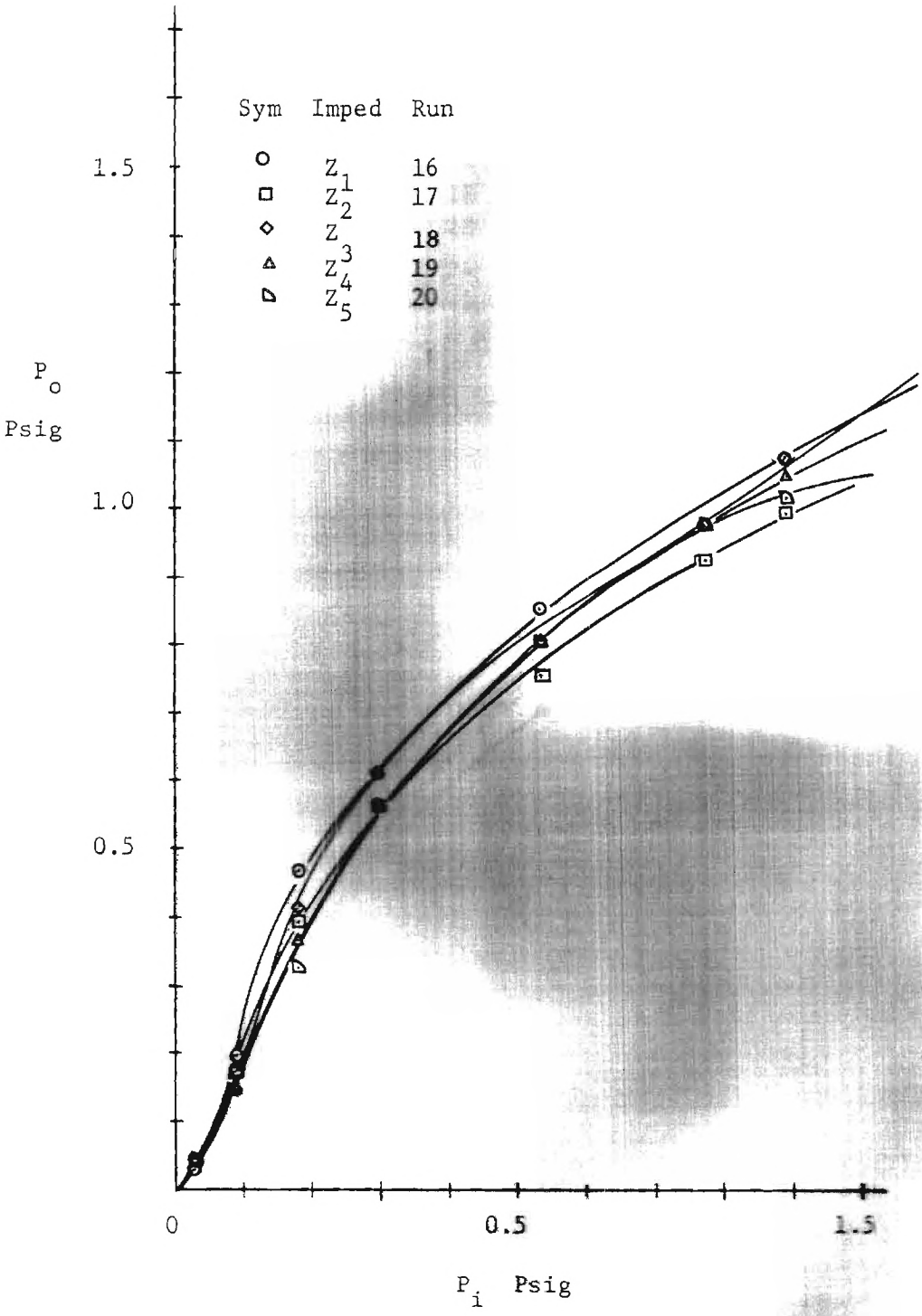

Figure 11. Output Pressure VS Input Pressure for $L/\ell = 6.04$, $P_s = 4$ psig

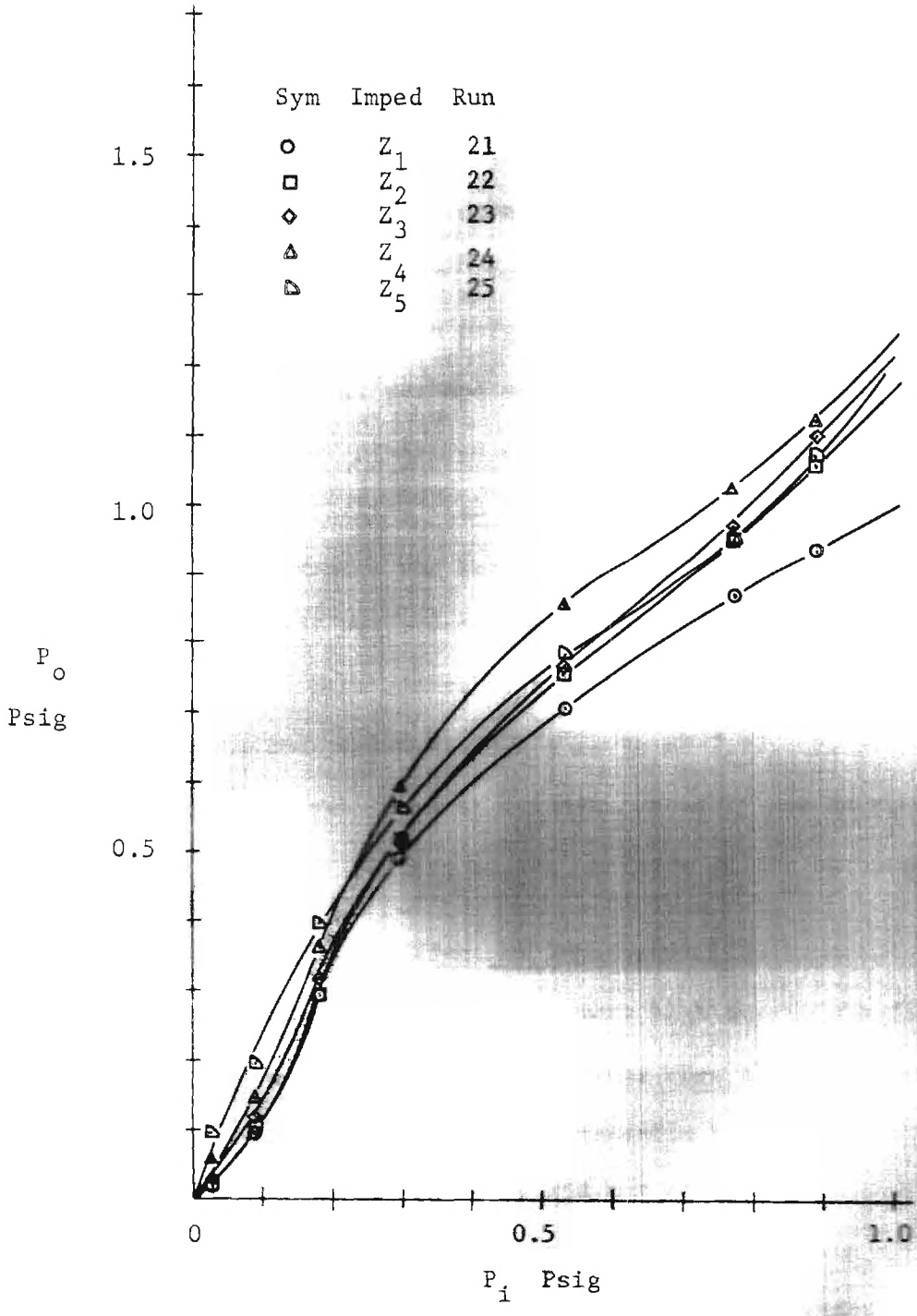

Figure 12. Output Pressure VS Input Pressure for $L/\ell = 8.00$, $P_s = 4$ psig

between L/ℓ ratios for various supply pressure combinations and at a prescribed impedance. Note that there appeared to be a peak ratio which produced the best performance near L/ℓ = 7.5.

As evidenced by Figures 8, 9, 10, 11, and 12, the performance of the DIM was improved with increase in supply pressure up to a point where the impact region became too unstable to set the initial conditions. As a result only four and six psig supplies were used. With increased accuracy of manufacture, perhaps some of the instability could be alleviated and thus higher pressures could be used. Figure 8 showed lower performance characteristics than Figure 9, both of which are at six psig supply. Performance was better with higher L/ℓ ratios. Figure 10 demonstrated the best performance of the four psig data, including Figures 11 and 12. Note generally that performance increased with output impedance and peaked at an L/ℓ ratio of 7.77. Behavior at the low input pressures was somewhat erratic, probably due to the marginal stability of the impact region at the entrance of the secondary plenum.

Effect of Impedance

Input impedance to the DIM was very high due to the flow rate required to maintain the initial conditions when the device was started. High input impedance was known to be desirable because of enhanced sensitivity (12). Output impedance did not affect the output pressure appreciabley as demonstrated in Figure 14, page 41. This effect seemed to be due to the fact that the back pressure caused by the additional impedance position the impact region to yield a fairly constant output pressure. Naturally, flow rate decreased as impedance increased as shown in Figure 15, page 43. For constant geometries and supply

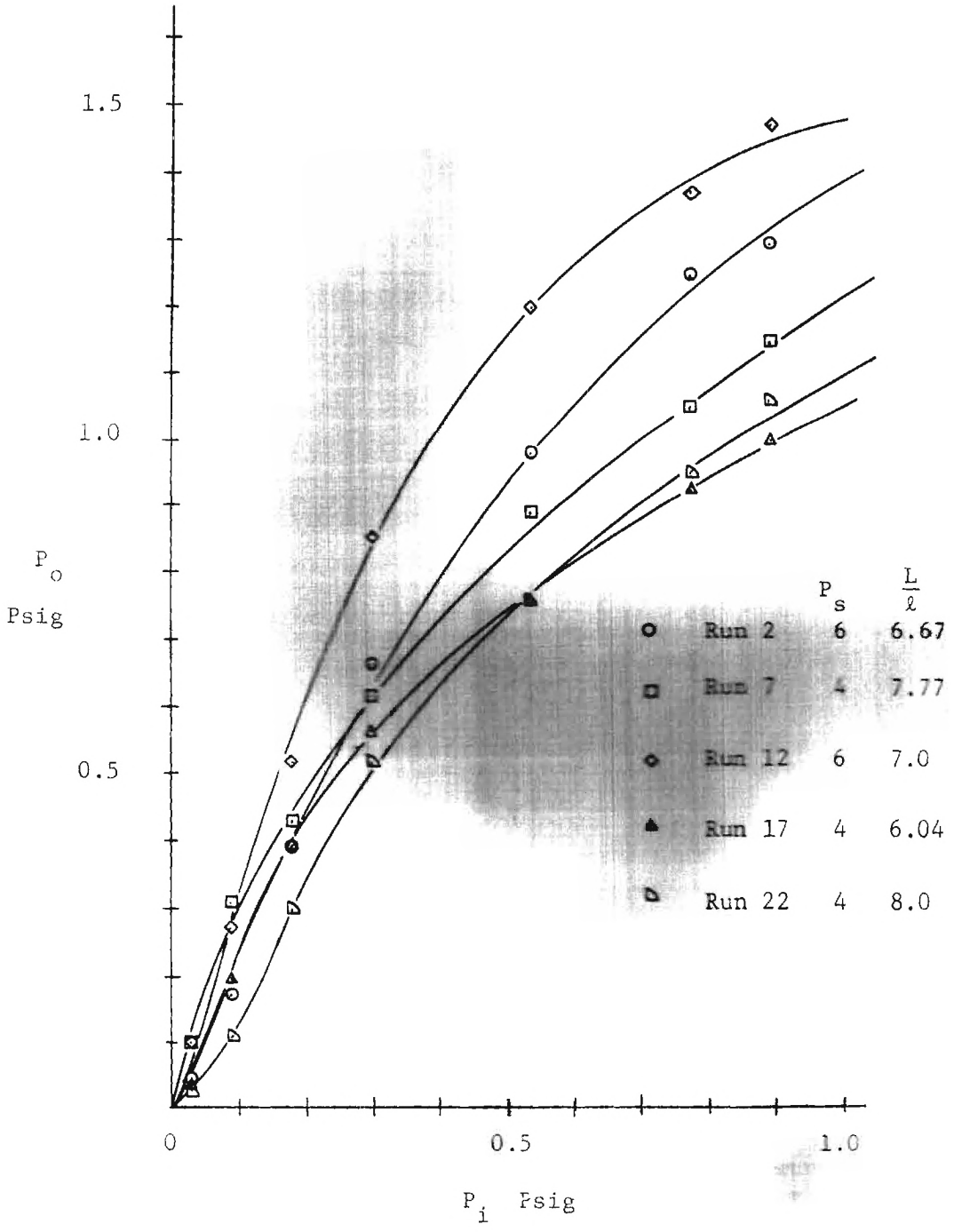

Figure 13. Output Pressure VS Input Pressure for Constant Output Impedance

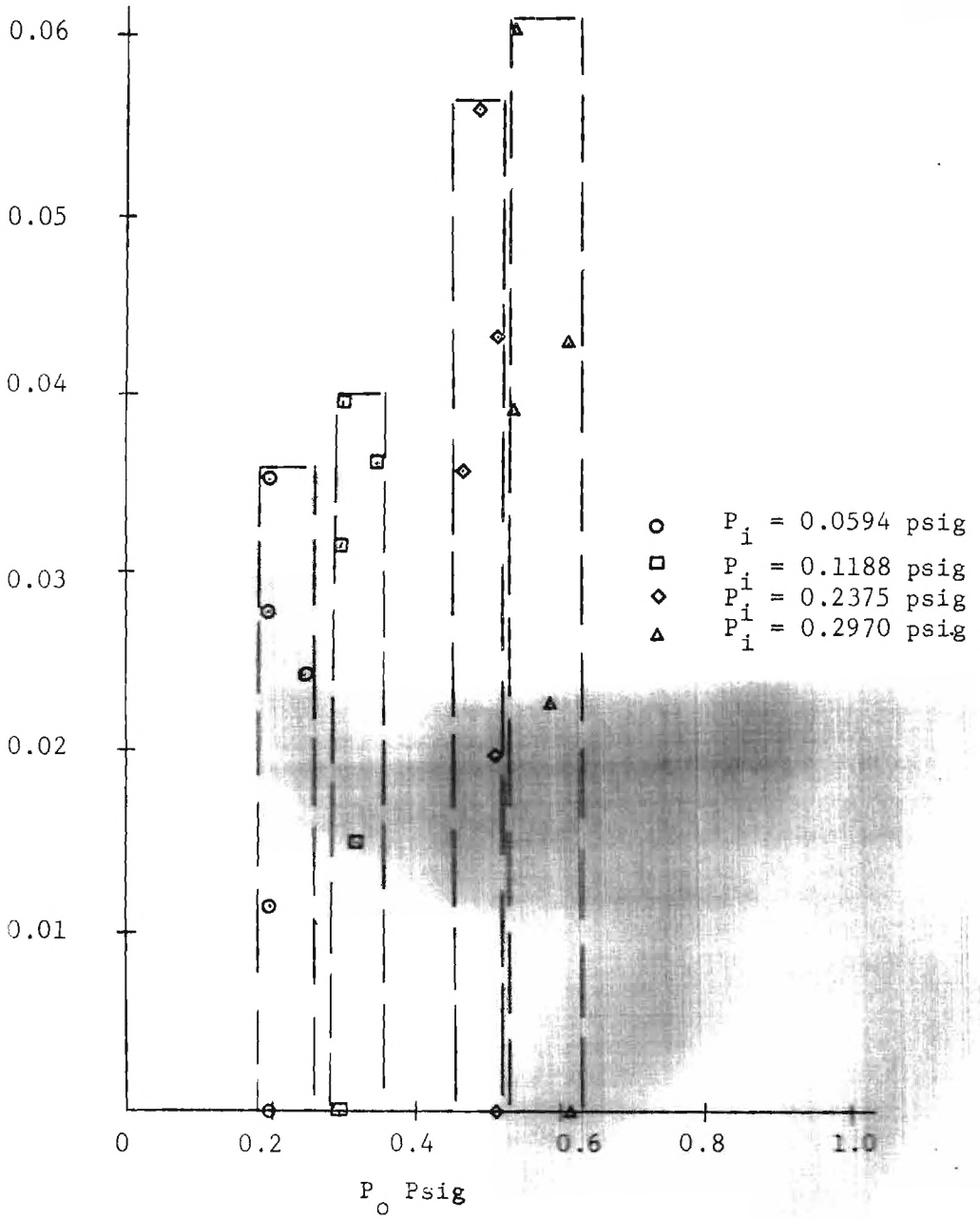

Figure 14. Output Flow Rate VS Output Pressure
P_s = 4 psig , L = 0.35 ℓ = 0.045
For Runs 6-10

pressures shown in Figure 15, the non-linearity of impedance due to the use of orifices was evident. Figure 16, page 44, demonstrated that output impedance, or more generally, input and ouput impedance, were not a function of the amplifier dynamic variables. The output impedance was constant and non-linear, within experimental error, for a variety of operating conditions. Data used in compiling the results may be found in Appendix C, Tables 6-10, pages 65-69.

One unusual effect was noted in the operation of the DIM. After setting the emitter supply and adjusting the input for atmospheric pressure, an oscillation of the impact region was observed as the collector pressure was increased. This periodic motion was caused when the impact region moved outside of the collector nozzle due to the collector supply pressure increase. At the same moment, a low pressure region in the collector secondary was formed by aspiration and drew the impact region back inside the plenum and the phenomenon repeated. This oscialiation increased in frequency as the collector supply pressure was increased, up to a threshold pressure where the impact region was stable. In every case, for this investigation, stability was attained at the initial conditions.

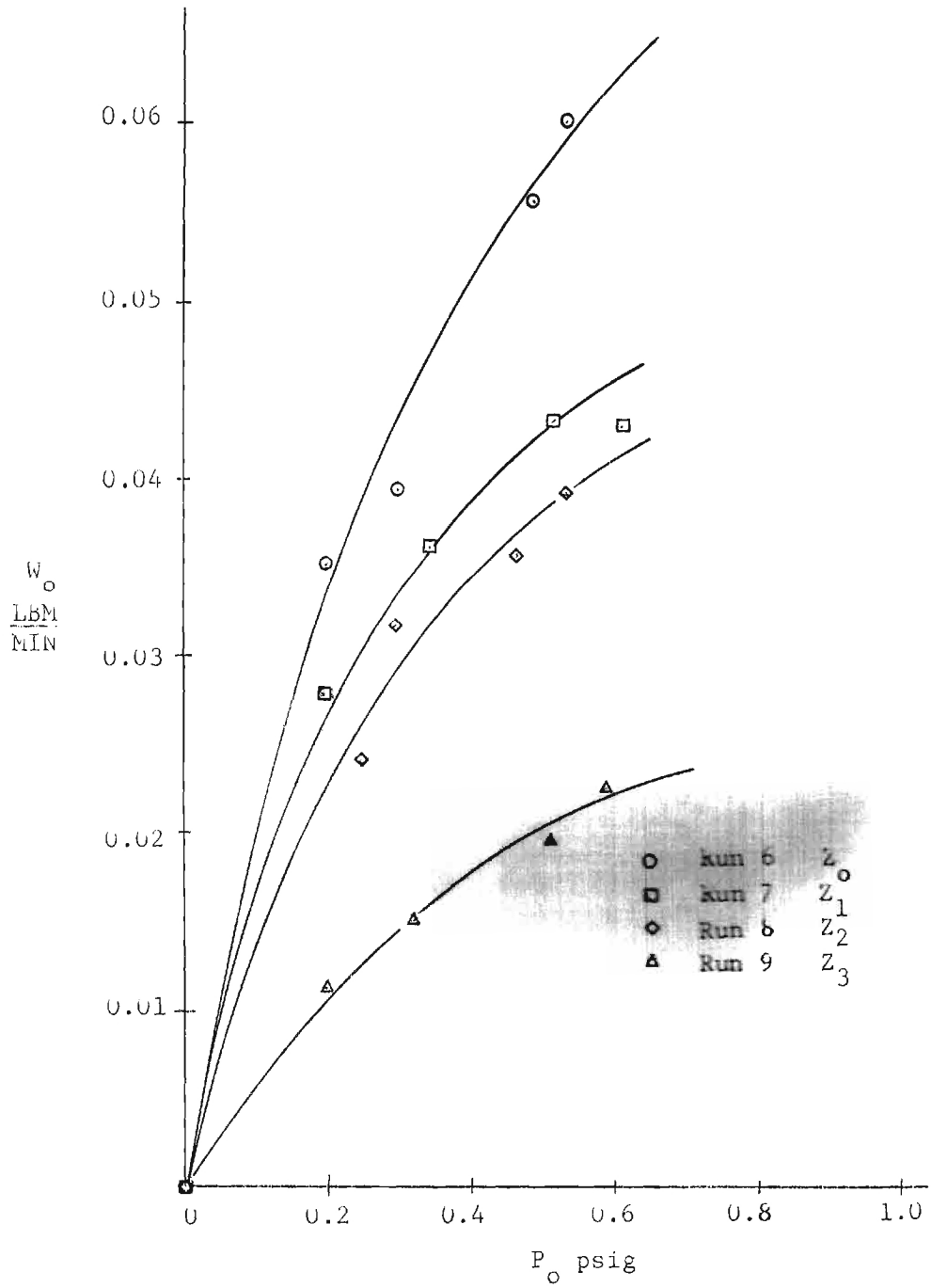

Figure 15. Output Flow Rate VS Output Pressure
P_s = 4 psig, L = 0.35, ℓ = 0.045

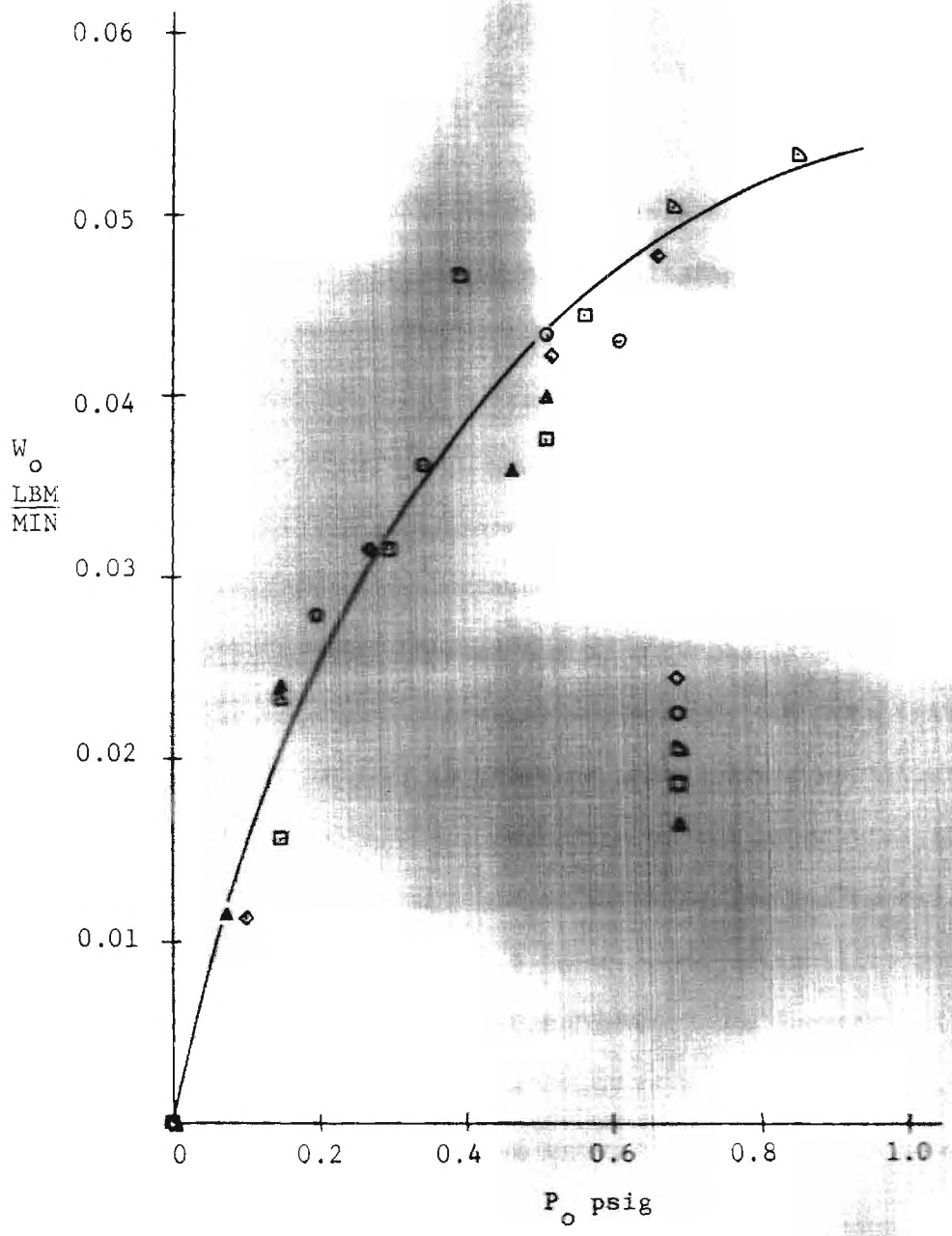

Figure 16. Output Flow Rate VS Output Pressure At Constant Output Impedance

CHAPTER V

CONCLUSIONS

Screw threads proved to be unacceptable as a means of nozzle alignment for this variable nozzle set; a sliding fit was found to be considerably more accurate. Alignment accuracy of both primary and secondary nozzles and of the two nozzle assemblies proved to be the most critical factor in the performance of the DIM. Pressure gains were much lower than expected evidently due to misalignment and manufacturing inaccuracies. An increase in flow rate might have improved the gain, but the flow was limited due to physical line constrictions.

Primary to secondary nozzle separation was the most sensitive geometric variable with respect to pressure gains; for a variation of 0.010 inches, the performance peaked. Secondary nozzle separation distances were less critical for pressure gains, but were limited by the attachment phenomenon at small distances --0.3 inches--and instability of the jet impact region at large distances--0.6 inches. The geometrical combination for the best pressure gain was found to be a primary-secondary separation distance of 0.045 inches and a secondary nozzle separation distance of 0.350 inches.

Performance generally improved with increase in supply pressure up to a point where the impact region was too unstable to establish the initial conditions. However the higher supply pressures increased the power consumption of the DIM. For maximum pressure gain in the DIM of

this investigation, four psig supply pressure yielded the best over-all results, although the six psig supply pressure provided higher output pressures for a certain range of input pressures. Generally, the higher supply pressures decreased the stability of the output.

Although pressure gains were somewhat disappointing, being about the same order of magnitude as for stream deflection amplifiers, flow gains were slightly higher. Pressure gains of three to four were experienced, while flow gains averaged eight to ten. The flow and pressure gain maximums for any one set of conditions occurred at different operating points.

One of the most outstanding contributions of this research was the prediction of physical dimensions of the DIM and their relation to the performance of the device. Unfortunately this information is deliberately omitted in contemporary literature for proprietary reasons.

CHAPTER VI

RECOMMENDATIONS

Tapering secondary nozzle faces were desirable to suppress the instability of the impact region due to the attachment phenomenon. Further refinements on the orifices could include drilling from both sides of the orifice to produce a sharp-edged aperture instead of a short tube as found in the nozzle set under consideration.

With the geometry established for maximum pressure gain as found in this investigation, a new configuration should be attempted. By machining the primary nozzle internally in a block of material, then fastening a face plate to close the chamber, both orifices could be drilled at once, and perfect alignment would be assured. Care should be taken to assure smooth internal surfaces to minimize boundary layer disturbances; the internal nozzle should have thin tapering walls for the same reason. Finally by mounting two of the nozzle assemblies on a two-dimensional traversing table, such as a milling machine bed, axial and angular alignment would be recommended, such as shining a concentrated light source through one set of orifices, reflecting the beam through the other set of orifices and then comparing coincidence of the two beams on a screen by way of half-silvered mirrors. The beam size should be the same size as the primary orifice and the reflecting mirror should be mounted perpendicular to the emitter reference base and on the rear face of the nozzle. The mirror system on the collector side should be

firmly attached to the stationary nozzle. Figure 23, page 61, of Appendix B, shows a cross-section of the proposed nozzle set and a schematic of the optical arrangement.

Once the geometry of the DIM was fixed, several investigations could be conducted to further establish operating characteristics. A transient analysis might be helpful to establish the relation of the output to the input with respect to phase lag, amplitude, and stability. This study would involve the use of electrical pressure transducers instead of manometers to permit rapid response. Also a sinusoidal generator in the form of a nozzle and wobble plate would be required in the input pressure line to provide a periodic signal.

Another test would investigate the possibility of using one supply for both emitter and collector primaries, and the use of a linear resistor between the collector primary and the common supply. This resistor would be sized such that the pressure drop through it would establish the impact region at the proper position in front of the collector nozzle to satisfy the initial conditions. Because of the linearity of the resistor, the impact region would remain established at the same point for a variety of supply pressures (13). Other investigations might include attempts at miniturization, operation in an enclosed environment, variation of nozzle diameters, stability analysis by mathematical modeling, signal to noise ratio, and velocity profile surveys.

The Direct Impact Modulator offered many possibilities for further study. The disadvantages of critical alignment, manufacturing accuracy, and stability should be more than compensated by the superior gain and adaptability to a variety of loads. As the operating characteristics

of the DIM, and impacting jets in general, are more fully explored. use of this new type of fluidic amplification in existing areas of application and in more exotic realms, should be limited only by the imagination of the designer.

APPENDIX A

CALCULATIONS

Upstream Pressure Maximum

It was necessary to determine what upstream pressure limit was possible for subsonic flow. Assuming that the supply pressure read on the gauge was stagnation pressure (p_o), that the exit pressure was atmospheric, and that the expansion was isentropic, the critical pressure ratio for air could be used to calculate the maximum upstream pressure. Although actual conditions varied somewhat from the ideal ones mentioned above, the result agreed well with that found in the literature (17).

$$\frac{p}{p_o} = 0.528 = \frac{14.7}{p_o}$$

$$p_o = 27.8 \text{ psia} = \underline{13.1 \text{ psig}}$$

By using supply pressures less than this value, subsonic flow would be assured.

Mass Flow Rate

Volumetric flow rate for compressible fluids was misleading unless the corresponding pressure was noted. Thus mass flow rate was a more reliable measure of flow. For air, an assumed ideal gas, the density was known to be a function of both temperature and pressure by the ideal gas law. But by noting the small range of absolute pressure change in

this research and the even smaller absolute temperature change. Variations in density due to pressure and temperature were negelected. As result, at a atmospheric pressure and 68°F,

$$\rho_{air} = 0.00234 \frac{\text{slugs}}{\text{ft}^3} = 0.0753 \frac{\text{lbm}}{\text{ft}^3}$$

$$\dot{w} = \rho Q \frac{\text{lbm}}{\text{min}}$$

where Q is the volumetric flow rate in cubic feet per minute.

Maximum ℓ Distance

Using the ideal model of a jet, Figure 1, page 3, and assuming negligible thickness of the secondary nozzle, uniform orifices, and symmetrical flow, the maximum distance for aspiration in the secondary plenum was determined (see Figure 17, page 52). If $\ell \geq \lambda$, then there would be a positive pressure in the input plenum, without an input, and the amplifier would not be operational. With reference to Figure 3, the potential core dended at $\frac{x}{D} = 5.2$, and at this point, the half-jet width was $\frac{y}{D} = 2.75$. Since d = 0.096 inches and D = 0.086 the maximum distance λ was found with the aid of similar triangles as shown in Figure 17:

5.2 (0.086) = 0.447 length to end of potential core

2.75 (0.086) = 0.236 half-jet width at end of potential core

$$\frac{0.005}{\lambda} = \frac{0.193}{0.447} \qquad \lambda = \underline{0.0116 \text{ inches}}$$

Therefore for $0 < \ell \leq 0.0116$ inches, aspiration should occur in the secondary plenum, theoretically.

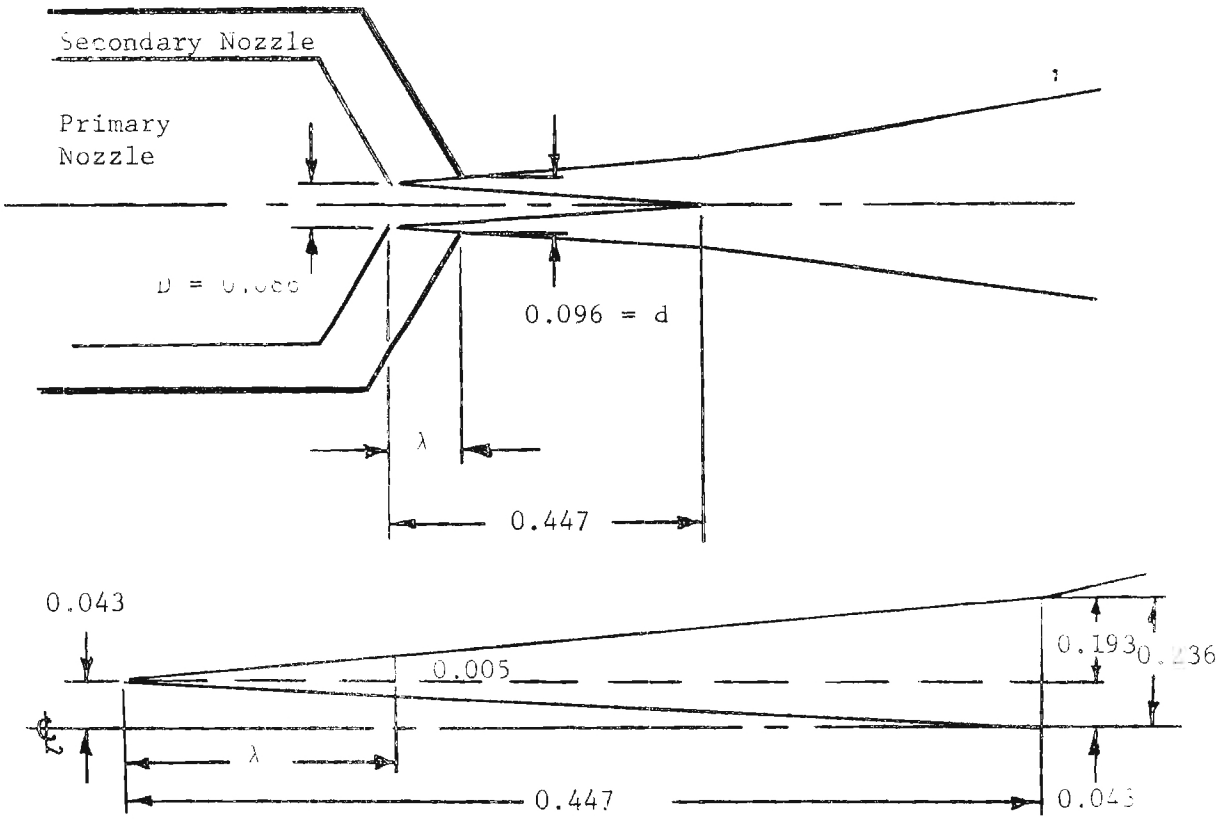

Figure 17. Jet Expansion from Command Nozzle

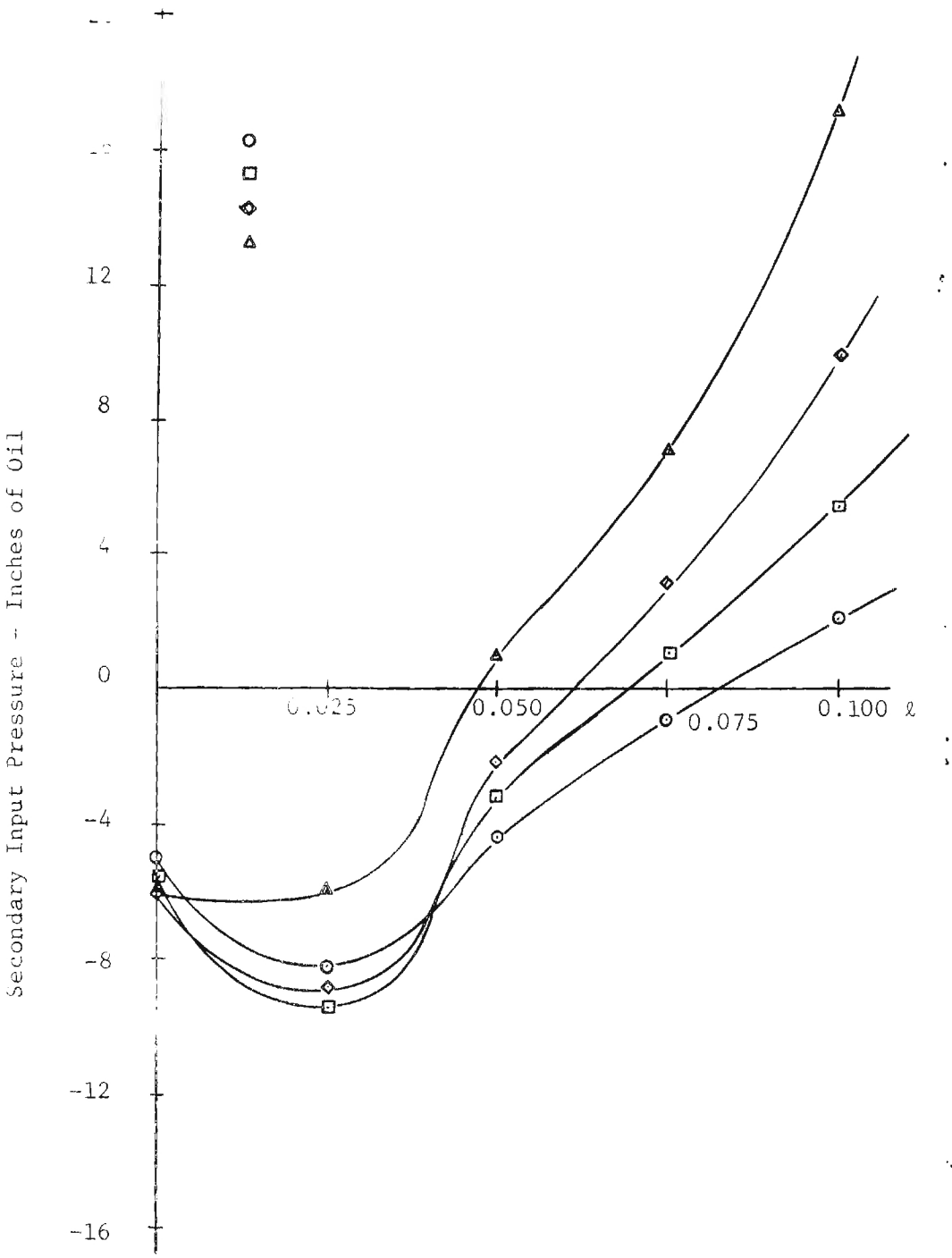

Figure 18. Emitter Nozzle Characteristics Configuration D Nozzles

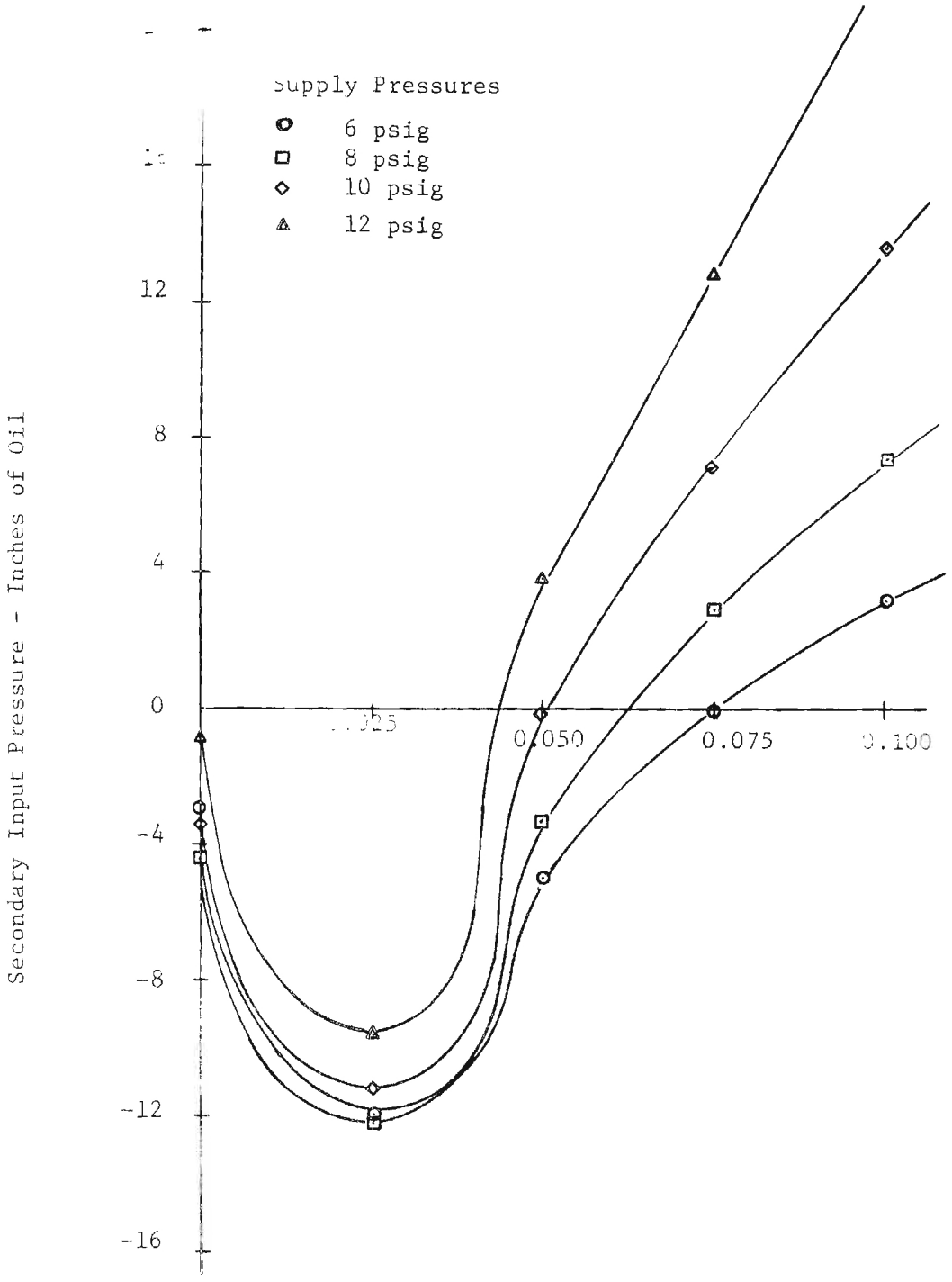

Figure 19. Collector Nozzle Characteristics Configuration D Nozzles

Associated with this test, was the preliminary nozzle survey to determine characteristics. Figures 18 and 19, pages 53 and 54, show similar although not identical characteristics. It should be noted that positive pressures occurred in the secondary for $\ell \geq 0.06$ inches on the average, dependent upon supply pressure. The discrepancy of this ℓ in comparison with the distance as found above was thought to be in the application of the ideal jet profile, irrespective of the supply pressure, and in nozzle inaccuracies.

Conversions

The output of the Meriam laminar flow elements was read on the inclined oil manometers for greater resolution in the small readings. Figure 20, page 56, shows the linear relation between the pressure read and standard flow rate in cubic feet per minute. Standard conditions were given as 14.73 psia and 60° Fahrenheit (16). To obtain the actual cubic feet per minute flow, the following relation was employed,

$$ACFM = SCFM \times \frac{14.73}{P} \times \frac{T}{530}$$

where SCFM was read from Figure 20, P was the absolute pressure in psia, and T was the absolute temperature in degrees Rankine for the flow under consideration. Other helpful conversions are given below.

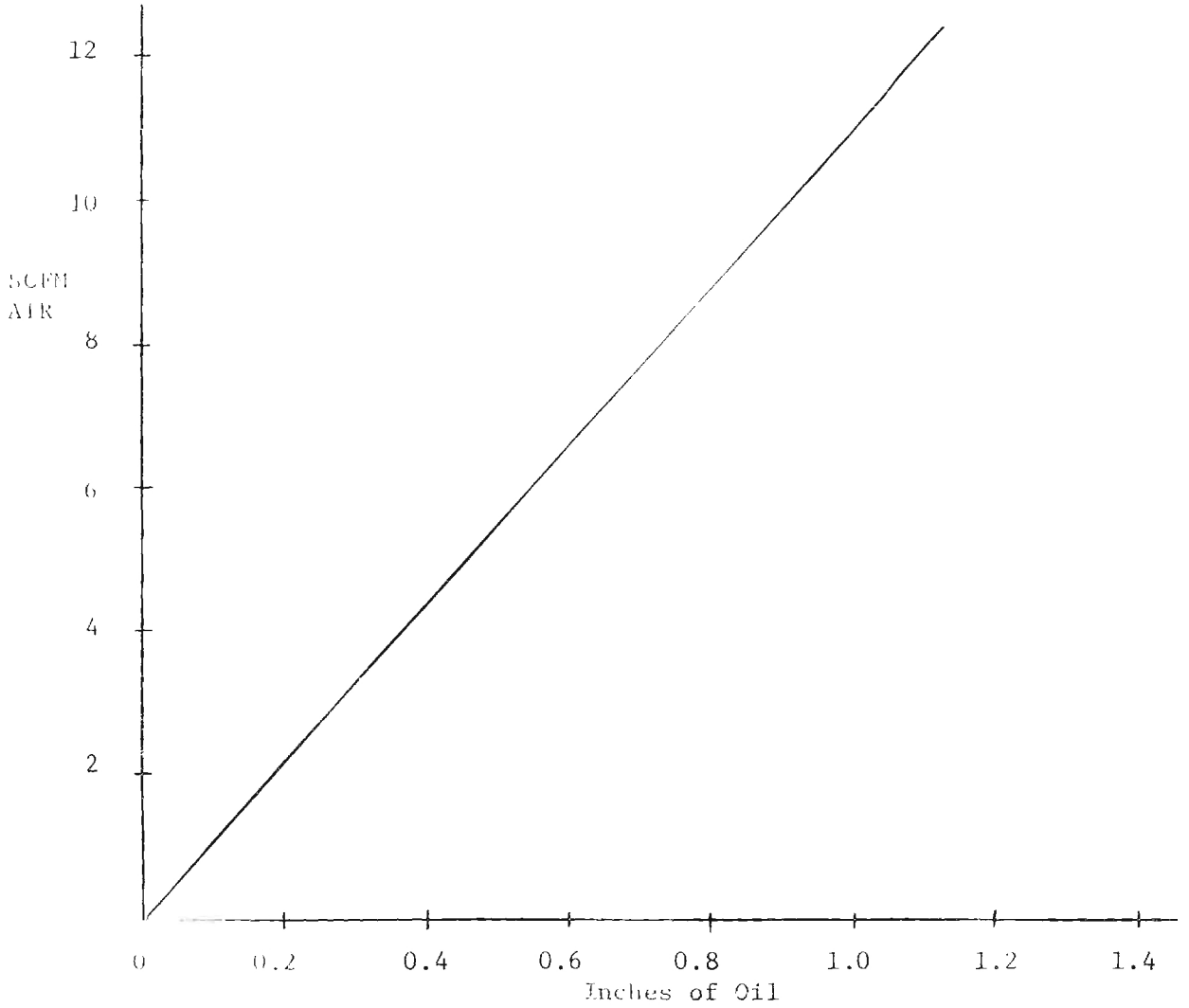

Figure 10. Conversion Chart for Laminar Flow Elements

1 inch Red Oil = 0.0297 psi

1 inch Mercury (Hg) = 0.4893 psi

(at 70°F)

APPENDIX B

SCHEMATICS

Following in Figures 21, 22, and 23, on pages 58, 59, and 60, are the construction details for Configuration A, Configuration D, and the proposed nozzle respectively. Figure 23 also shows a suggested optical alignment procedure to rectify the most critical error in this investigation--nozzle alignment. Figure 24, page 61, shows the detail of the one-dimensional traversing mechanism for supporting the nozzles. In Figure 25, page 62, is shown the fluid circuit for the test stand.

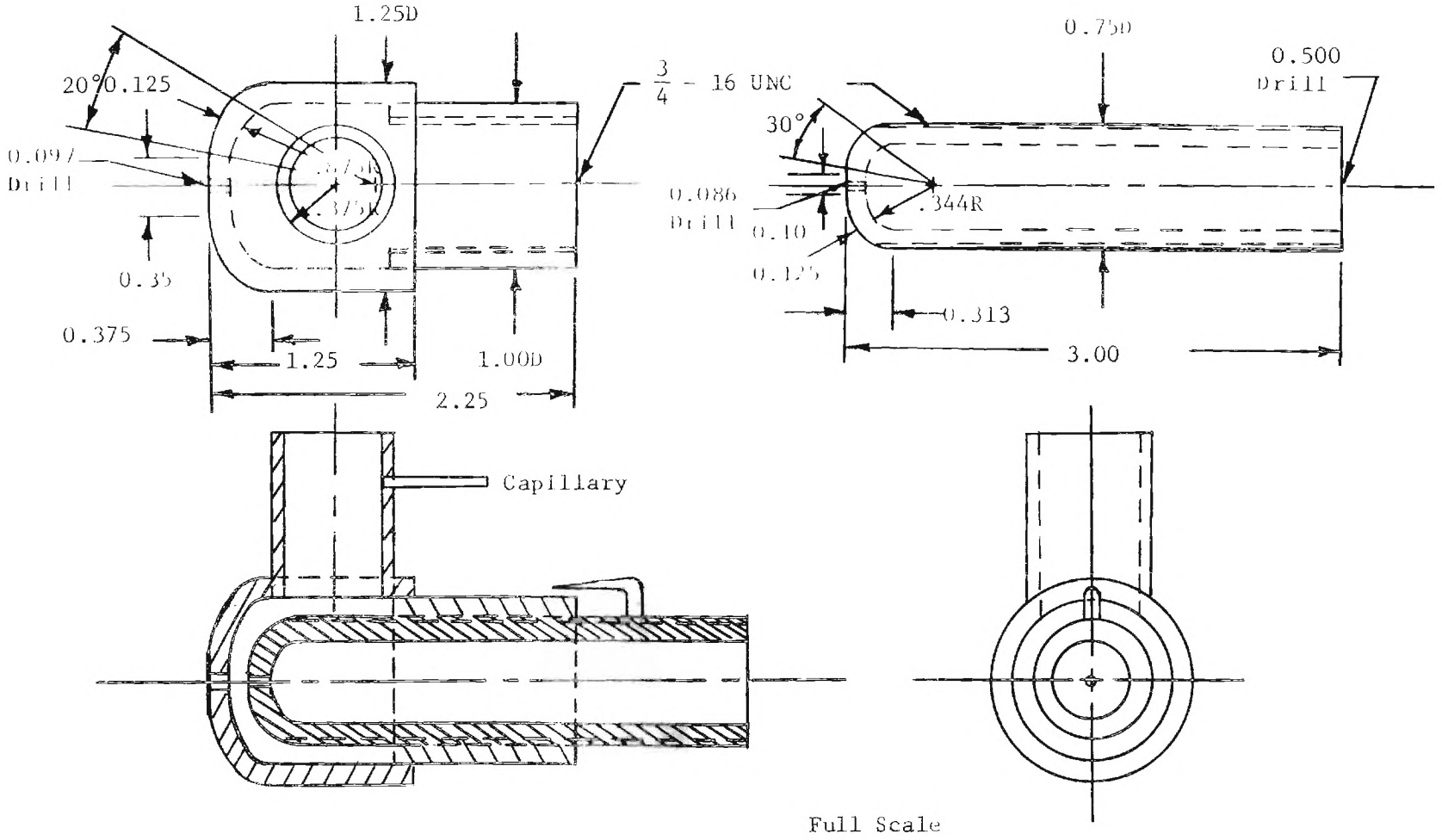

Figure 21. Configuration A Nozzle Assembly Detail

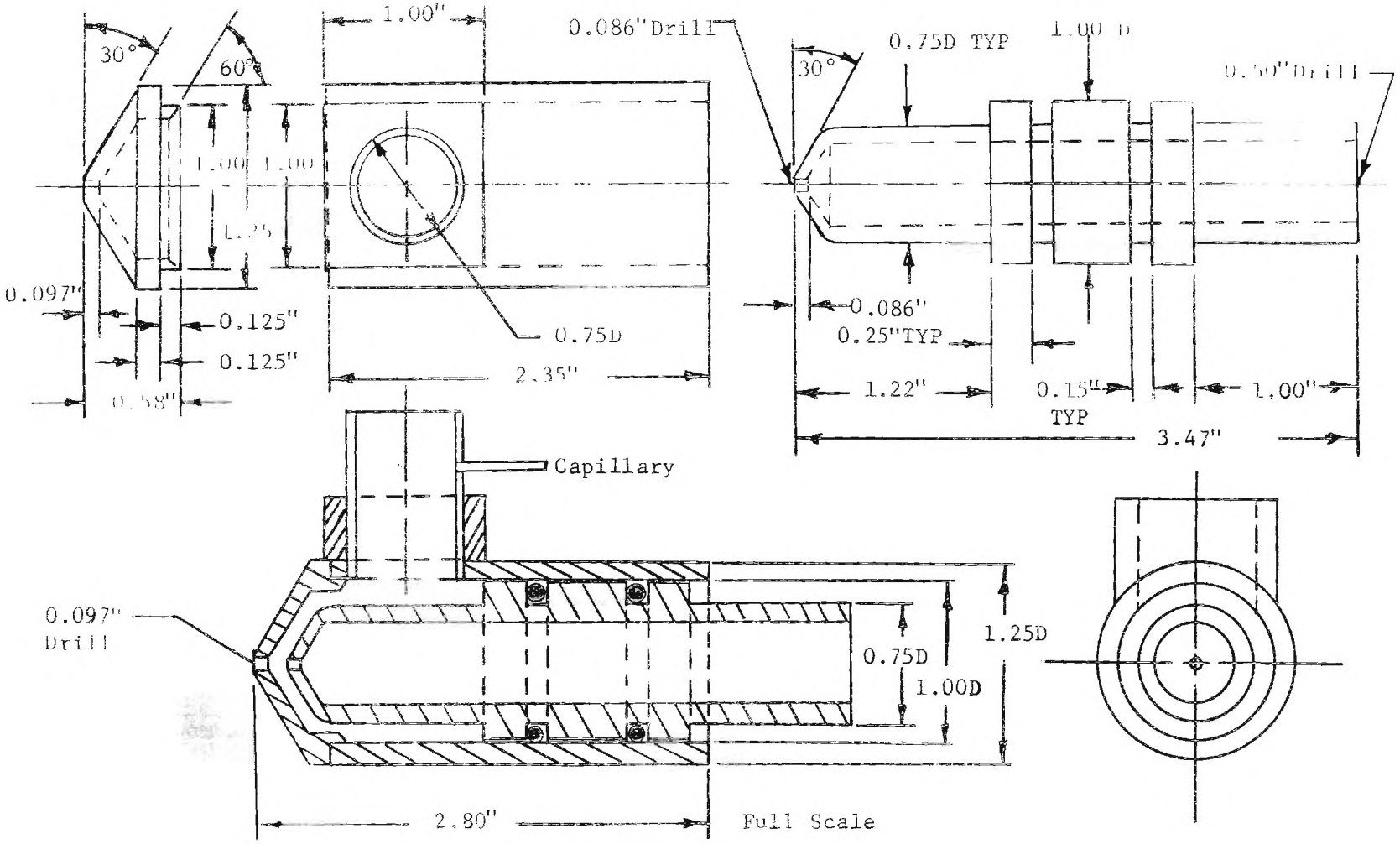

Figure 22. Configuration D Nozzle Assembly Detail

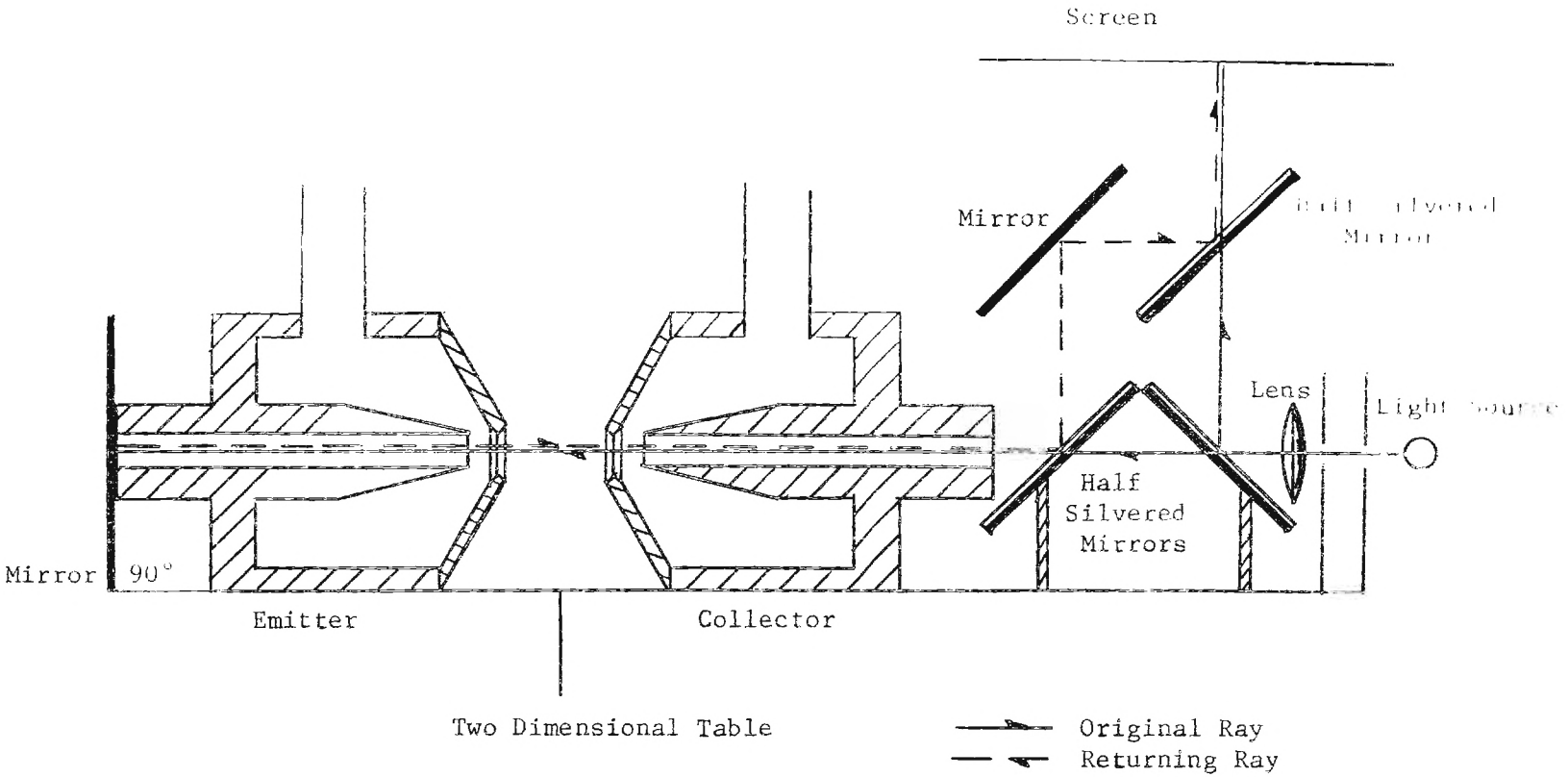

Figure 23. Recommended Nozzle Configuration (With Alignment Procedure Shown)

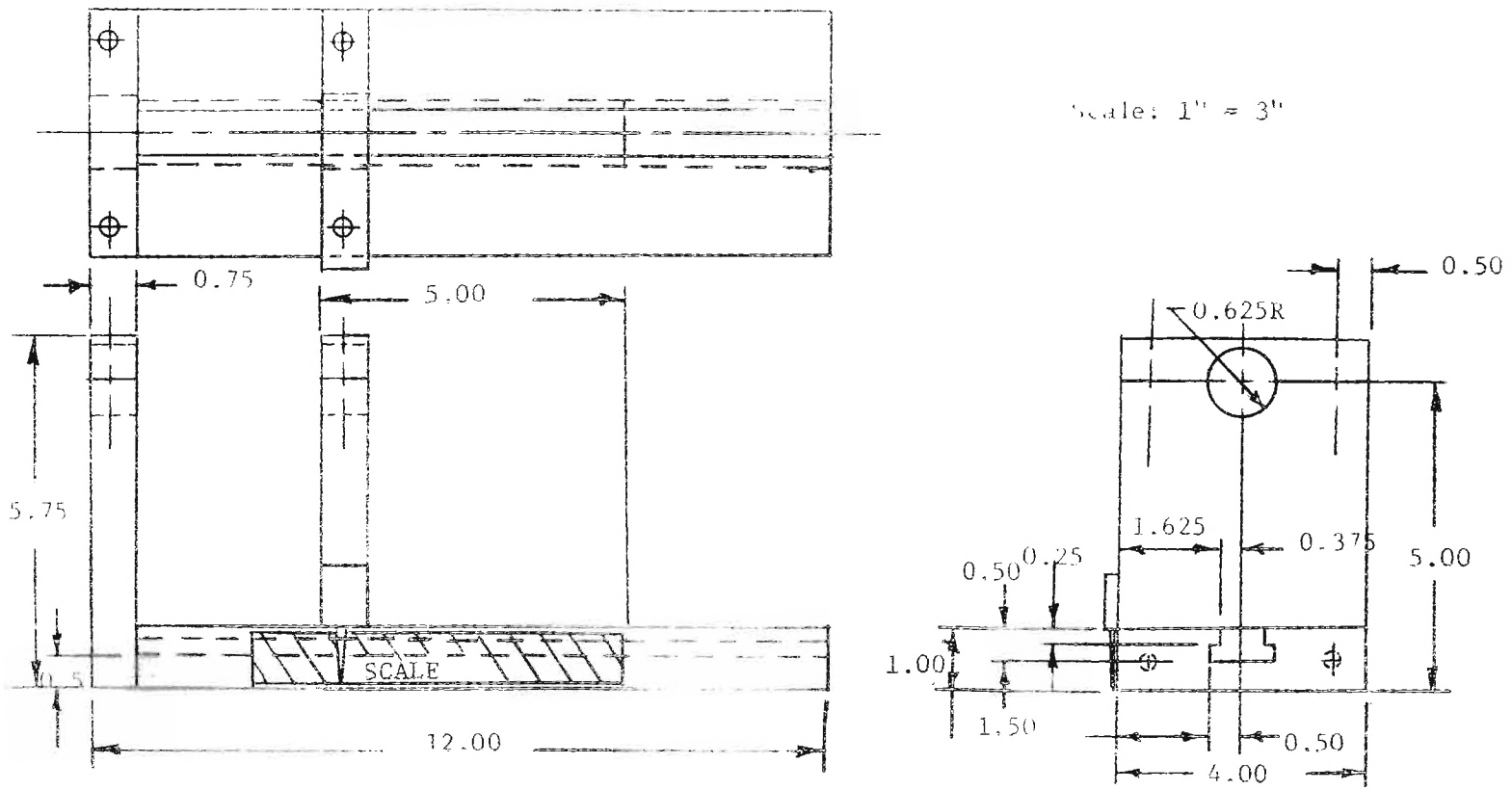

Figure 24. Trimming Mechanism

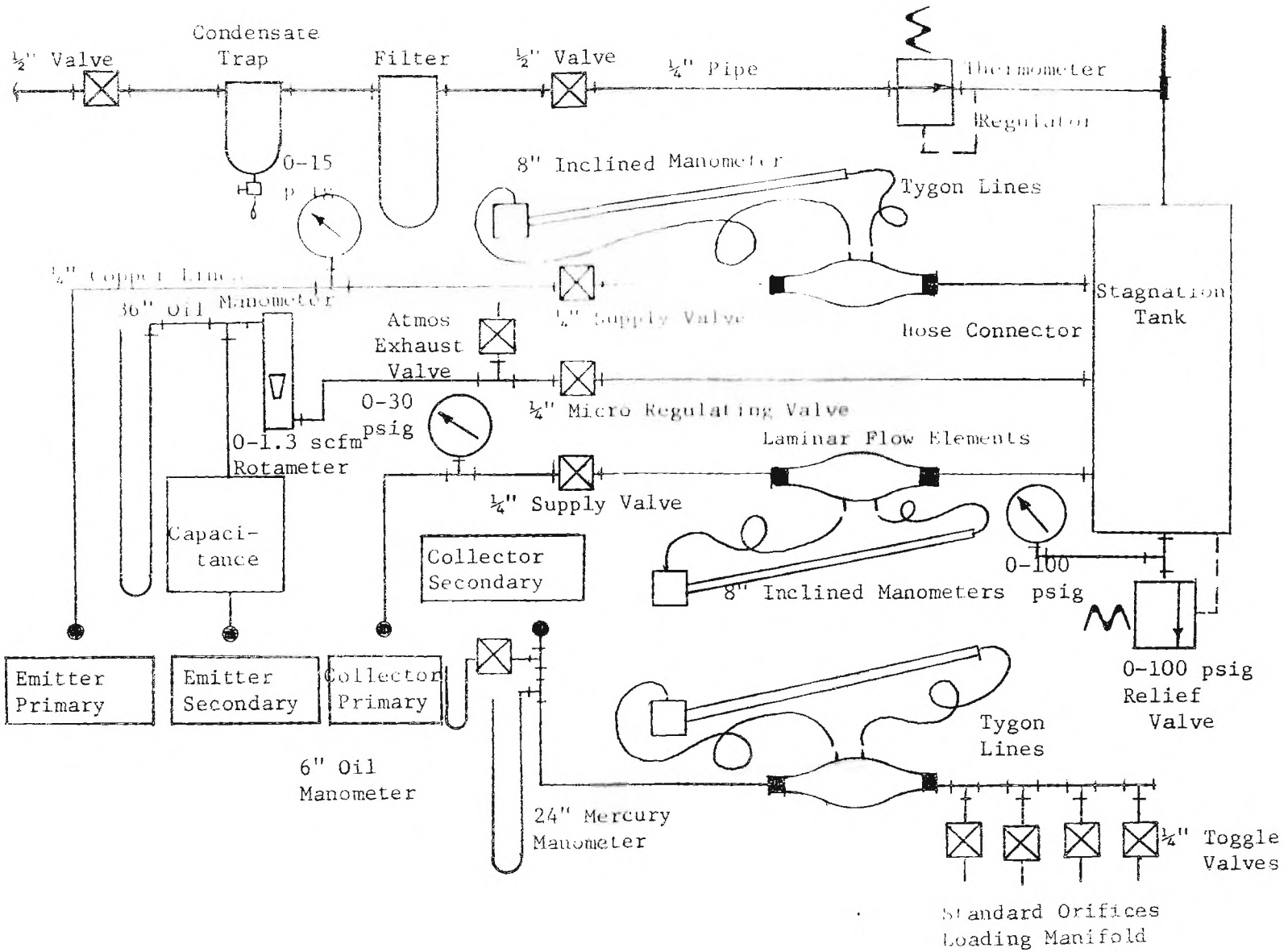

Figure 25 Fluid Circuit Schematic

APPENDIX C

DATA

Following in Tables 6, 7, 8, 9, and 10, are the rough data used in developing the graphs and tables in this investigation.

Table 6. Block IV Rough Data-Runs 1-5
T = 72°F

Run No. Conditions	Pe	Pc	in Ws /oil*	in Pi /oil	Wi SCFM	in Po /Hg	Wo /oil
1	5.8	5.5	0.064	2	0.075	0.20	0.030
Z_0	5.8	5.5	0.064	4	0.090	0.45	0.050
P = 8 psig	5.9	5.6	0.064	6	0.110	0.90	0.060
λ = 0.045	5.9	5.6	0.064	8	0.120	1.25	0.070
L = 0.30	5.9	5.6	0.064	10	0.135	1.45	0.080
2	5.9	5.6	0.064	2	0.070	0.20	0.015
Z_1	5.9	5.6	0.064	4	0.090	0.55	0.040
	5.9	5.6	0.064	6	0.100	0.80	0.050
	5.9	5.6	0.064	8	0.120	1.05	0.055
	6.0	5.75	0.064	10	0.135	1.35	0.060
3	5.9	5.7	0.064	2	0.070	0.20	0.015
Z_2	5.9	5.7	0.064	4	0.085	0.45	0.025
	5.9	5.7	0.064	6	0.105	0.80	0.030
	5.9	5.7	0.064	8	0.120	0.95	0.040
	5.9	5.7	0.064	10	0.135	1.15	0.045
4	5.5	5.5	0.064	2	0.065	0.30	0.010
Z_3	5.8	5.5	0.064	4	0.085	0.50	0.015
	5.85	5.6	0.064	6	0.100	0.80	0.015
	5.9	5.7	0.064	8	0.115	1.00	0.020
	5.9	5.7	0.064	10	0.130	1.20	0.025
5	5.8	5.5	0.064	2	0.070	0.30	0
Z_4	5.8	5.7	0.064	4	0.080	0.60	
	5.9	5.8	0.064	6	0.100	0.80	
	5.9	5.8	0.064	8	0.110	1.00	
	6.0	5.9	0.064	10	0.130	1.20	

*See Figure 20 page 56

Table 7 Rough Data-Runs 6-10
T = 73°F

Run No. Conditions	Pe	Pc	in Ws /oil	in Pi /oil	Wi SCFM	in Po /Hg	in Wo /oil
	3.95	3.4	0.052	2	0.045	0.40	0.045
Z_o	3.95	3.4	0.052	4	0.060	0.60	0.050
P_s = 4psig	3.95	3.4	0.052	6	0.080	0.80	0.060
Z_s = 0.045	4.10	3.6	0.052	8	0.100	1.00	0.070
L = 0.35	4.15	3.6	0.052	10	0.110	1.10	0.075
7	3.95	3.35	0.051	2	0.065	0.40	0.035
Z_1	3.95	3.4	0.051	4	0.080	0.70	0.045
	4.0	3.5	0.051	6	0.100	0.87	0.050
	4.0	3.5	0.051	8	0.120	1.05	0.055
	4.05	3.6	0.051	10	0.140	1.25	0.055
8	3.85	3.25	0.049	2	0.070	0.50	0.030
Z_2	3.9	3.3	0.049	4	0.080	0.60	0.040
	4.0	3.4	0.049	6	0.110	0.70	0.045
	4.1	3.5	0.049	8	0.130	0.95	0.045
	4.1	3.5	0.049	10	0.150	1.10	0.050
9	4.0	3.4	0.050	2	0.065	0.40	0.015
Z_3	4.0	3.5	0.050	4	0.090	0.65	0.020
	4.1	3.6	0.050	6	0.110	0.90	0.020
	4.15	3.7	0.050	8	0.120	1.05	0.025
	4.2	3.75	0.050	10	0.140	1.20	0.028
10	3.9	3.5	0.050	2	0.070	0.40	0
Z_4	4.0	3.6	0.050	4	0.085	0.60	
	4.05	3.65	0.050	6	0.105	0.85	
	4.1	3.7	0.050	8	0.120	1.05	
	4.15	3.75	0.050	10	0.140	1.25	

Table 8 Rough Data-Runs 11-15
T = 72°F

Run No. Conditions	Pe	Pc	Ws in /oil	Pi in /oil	Wi SCFM	Po in /Hg	Wo in /oil
11	5.9	5.0	0.062	2	0.065	0.05	0.010
Z_o	5.9	5.0	0.062	4	0.080	0.25	0.030
P_s = 6psig	6.0	5.1	0.062	6	0.100	0.55	0.040
ℓ_s = 0.050	6.05	5.2	0.062	8	0.110	0.95	0.060
L = 0.35	6.1	5.25	0.062	10	0.120	1.25	0.080
12	5.8	4.75	0.061	2	0.065	0.30	0.030
Z_1	5.85	4.8	0.061	4	0.085	0.80	0.060
	5.9	4.9	0.061	6	0.100	1.05	0.060
	5.9	4.9	0.061	8	0.110	1.40	0.065
	5.9	5.0	0.061	10	0.120	1.75	0.070
13	5.9	5.05	0.062	2	0.065	0.10	0.007
Z_2	6.0	5.1	0.062	4	0.080	0.30	0.020
	6.05	5.2	0.062	6	0.095	0.55	0.030
	6.05	5.2	0.062	8	0.110	0.85	0.035
	6.05	5.2	0.062	10	0.120	1.05	0.040
14	5.8	4.7	0.063	2	0.060	0.30	0.015
Z_3	5.8	4.8	0.063	4	0.080	0.70	0.020
	5.8	4.9	0.063	6	0.095	1.05	0.025
	5.8	5.0	0.063	8	0.110	1.45	0.030
	5.85	5.1	0.063	10	0.120	1.70	0.030
15	5.9	4.9	0.061	2	0.060	0.30	0
Z_4	6.0	5.0	0.061	4	0.080	0.70	[illegible]
	6.0	5.1	0.061	6	0.090	1.05	[illegible]
	6.0	5.2	0.061	8	0.110	1.55	[illegible]
	6.05	5.3	0.061	10	0.120	1.70	[illegible]

Table 9 Rough Data-Runs 16-20
T = 72°F

Run No. Conditions	Pe	Pc	in Ws /oil	in Pi /oil	Wi SCFM	in Po /Hg	in Wo /oil
16	3.95	3.3	0.051	2	0.070	0.30	0.030
Z_0	3.95	3.3	0.051	4	0.090	0.55	0.050
P_s = 4psig	4.0	3.4	0.051	6	0.110	0.95	0.055
ℓ^s = 0.055	4.0	3.4	0.051	8	0.130	1.05	0.060
L = 0.35	4.1	3.5	0.051	10	0.150	1.25	0.070
17	3.95	3.3	0.050	2	0.070	0.30	0.020
Z_1	3.95	3.3	0.050	4	0.090	0.60	0.040
	4.0	3.4	0.050	6	0.110	0.80	0.045
	4.1	3.5	0.050	8	0.130	1.05	0.050
	4.15	3.6	0.050	10	0.140	1.15	0.055
18	4.0	3.3	0.050	2	0.070	0.20	0.015
Z_2	4.1	3.4	0.050	4	0.085	0.55	0.030
	4.1	3.4	0.050	6	0.110	0.85	0.035
	4.15	3.5	0.050	8	0.120	1.05	0.040
	4.15	3.6	0.050	10	0.140	1.25	0.045
19	4.0	3.3	0.050	2	0.065	0.20	0.007
Z_3	4.0	3.3	0.050	4	0.085	0.50	0.015
	4.05	3.4	0.050	6	0.105	0.75	0.018
	4.05	3.4	0.050	8	0.120	1.05	0.020
	4.1	3.5	0.050	10	0.140	1.15	0.020
20	3.9	3.1	0.051	2	0.065	0.20	0
Z_4	3.95	3.25	0.051	4	0.085	0.45	0
	4.0	3.35	0.051	6	0.100	0.67	0
	4.05	3.5	0.051	8	0.120	0.90	0
	4.15	3.6	0.051	10	0.140	1.15	0

Table 10 Rough Data-Runs 21-25
T = 75°F

Run No. Conditions	Pe	Pc	in Ws /oil	in Pi /oil	Wi SCFM	in Po /Hg	in Wo /oil
21	3.9	3.05	0.051	2	0.060	0.10	0.015
Z_o	3.9	3.05	0.051	4	0.080	0.30	0.040
P_s = 4psig	4.0	3.1	0.051	6	0.100	0.60	0.050
ℓ_s = 0.050	4.0	3.2	0.051	8	0.120	0.80	0.060
L = 0.40	4.1	3.25	0.051	10	0.140	1.00	0.070
22	4.0	3.05	0.050	2	0.070	0.15	0.015
Z_1	4.0	3.05	0.050	4	0.090	0.30	0.030
	4.05	3.1	0.050	6	0.110	0.60	0.035
	4.1	3.25	0.050	8	0.125	0.95	0.045
	4.1	3.25	0.050	10	0.140	1.05	0.050
23	3.9	3.0	0.051	2	0.070	0.15	0.010
Z_2	3.9	3.0	0.051	4	0.085	0.35	0.020
	4.0	3.1	0.051	6	0.110	0.65	0.030
	4.0	3.1	0.051	8	0.120	0.85	0.035
	4.1	3.25	0.051	10	0.140	1.05	0.040
24	3.9	3.0	0.051	2	0.065	0.20	0.010
Z_3	4.0	3.1	0.051	4	0.080	0.55	0.015
	4.05	3.2	0.051	6	0.100	0.75	0.015
	4.1	3.35	0.051	8	0.120	1.00	0.015
	4.2	3.5	0.051	10	0.135	1.22	0.020
25	4.0	3.2	0.050	2	0.070	0.30	0
Z_4	4.1	3.3	0.050	4	0.095	0.55	0
	4.1	3.3	0.050	6	0.110	0.80	0
	4.2	3.5	0.050	8	0.120	1.00	0
	4.2	3.5	0.050	10	0.140	1.15	0

BIBLIOGRAPHY

1. Hunter Rouse and Simon Inc., History of Hydraulics, Dover Publications, Inc., New York, 1963, pp. 47, 66.

2. Ascher H. Shapiro, The Dynamics and Thermodynamics of Compressible Fluid Flow, Ronald Press Company, New York, 1953.

3. Kenneth W. Misevich, "The Impact of Opposing Axially Symmetric Jets", Advances in Fluidics, American Society of Mechanical Engineers, 1967, p. 98 ff.

4. W. B. Benton, A Fluidic Impact Modulation Test System, Undergraduate Project Report, Georgia Institute of Technology, School of Mechanical Engineering, 1967.

5. G. N. Abramovich, The Theory of Turbulent Jets, The MIT Press, Cambridge, 1963.

6. S. Goldstein, editor, Modern Developments in Fluid Dynamics, Dover Publications, Inc., vol. II, p. 592 ff.

7. A. K. Simson, A Theoretical Study of the Design Parameters of Subsonic Pressure Controlled, Fluid Jet Amplifiers, Thesis (Ph.D.) Department of Mechanical Engineering, Massachusetts Institute of Technology, July 15, 1963.

8. Forbes T. Brown and Anton K. Simson, "The Power Jet Representation", Research in Pressure-Controlled Fluid Jet Amplifiers, U. S. Army Missile Command, Redstone Arsenal, Alabama, 1963, p. 10 ff.

9. Hunter Rouse, editor, Advanced Mechanics of Fluids, John Wiley and Sons, Inc., New York, 1965, p. 383.

10. T. J. Lechner and P. H. Sorenson, "Some Properties and Applications of Direct and Transverse Impact Modulators", Proceedings of the Fluid Amplification Symposium, Harry Diamond Laboratories, 1964, vol. II, p. 34 ff.

11. E. F. Humphrey and D. H. Tarumoto, Fluidics, Fluid Amplifier Associates, 1964, p. 34 ff.

12. B. G. Bjornsen, "The Impact Modulator", Proceedings of the Fluid Amplification Symposium, Harry Diamond Laboratories, 1964, vol. II, p. 5 ff.

13. B. G. Bjornsen, "A Fluid Amplifier Pneumatic Controller", Control Engineering, vol. XII, June 1965, p. 88 ff.

14. H. L. Fox and O. L. Wood, "Fluid Amplifiers-- The Development of Basic Devices and the Need for Theory", Control Engineering, September 1964, p. 75 ff.

15. D. L. Letham, "Fluidic System Design", Machine Design 1966 reprint, vol. II, p. 20.

16. Meriam Instrument Company, "Meriam Laminar Flow Element Model 50-MC2", Technical Note 2A, p. 3.

17. Kenneth W. Misevich, "Visualization of the Impacting Air Jets", Supplement to the author's paper, The Impact of Opposing Axially Symmetric Jets (3), Johnson Service Company, 1967.